Singh. Arch Addict Rehabil 2017, 1(2):56-82
DOI: 10.36959/843/424 | Volume 1 | Issue 2

Review Article Open Access

Critical Review of Alcohol, Alcoholism and the Withdrawal Symptoms-III. An Introduction to Nanoparticles and their Applications in Alcoholism Treatment

Ashok K Singh*

Department of Veterinary Population Medicine, College of Veterinary Medicine, University of Minnesota, USA

Abstract

Alcoholism is a complex heterogeneous disease with many contributing factors that may vary from person to person, and are known to have a major impact on treatment outcome. Thus, a single treatment strategy may not work for everyone, stressing an urgent need to develop personalized treatments based on the person's genetic and environmental factors. Recent advancements in nanotechnology have allowed construction of unique Nanoparticles (NPs) having potentials for personalized treatments by: (i) Delivering Therapeutic Drugs (TDs) to specific sites, (ii) Releasing TDs on-demand by internal or external cues, and (iii) Serving as vectors for transfection of cDNA-plasmids into the host's gene to increase the gene expression and/or siRNA to inhibit the gene expression.

There are substantial, but not compelling evidence for application of Engineered NPs (ENPs) on screening and treatment of alcoholism. The key factor that confers the ENPs their unique therapeutic potency is that, irrespective of differences in their composition, ENPs exhibit some common unique physicochemical properties (such as high surface area to volume ratio, high surface reactivity that is inversely related to the size, and unique electronic, optical and magnetic properties) not found in bulk particles. The therapeutic potency/toxicity ratio of an ENP may determine its therapeutic index, possibly because the physicochemical characteristics that confer the ENPs their unique properties are also responsible for their toxicity. Therefore, the aims of this review are to discuss (1) The ENPs' structure, physicochemical properties, beneficial properties and toxicity, and (2) Their relevance in development if individualized treatment against alcoholism.

Keywords

Nanoparticles, Clusters, Nanotechnology, Nanotoxicology, Bulk particles, Surface molecules, Surface area and volume ratio, Metals, Semiconductors, Magnetism, Dendrimers, Isotropic, Anisotropic, Precautionary principle.

Introduction

Alcoholism is a chronic, multifaceted disorder in which the gene-environment interactions play a key role in the disease's etiology [1,2]. The consequences of alcohol abuse that results in development of alcoholism have been attributed to the alcohol's toxic effects on the brain [3]. Figure 1 shows several neurobiological circuits that are central to different stages of addiction [4-11] (Figure 1).

Different neurotransmitter systems targeted by alcohol are GABA [12,13], glutamate [14], serotonin [15], nor epinephrine [16], neuropeptide Y [17], vasopressin [18], adenosine [19] and Dopamine (DA) [2,20-22]. Because of (i) The mechanistic complexities of alcoholism [23] and (ii) Diverse interaction of genetically differently people to their environment, the current common therapy consisting of a combination of psychological, behavioral and pharmacological approaches exhibits high individual variability in treatment outcomes including high incidence of relapse. Therefore development of an individualized, patient-specific treatment strategy is highly desirable.

***Corresponding author:** Ashok K Singh, Department of Veterinary Population Medicine, College of Veterinary Medicine, University of Minnesota, St Paul, MN 55108, USA, Tel: 612-625-6782, E-mail: singh001@umn.edu

Received: February 01, 2017; **Accepted:** July 08, 2017; **Published online:** July 10, 2017

Citation: Singh AK (2017) Critical Review of Alcohol, Alcoholism and the Withdrawal Symptoms-III. An Introduction to Nanoparticles and their Applications in Alcoholism Treatment. Arch Addict Rehabil 1(2):56-82

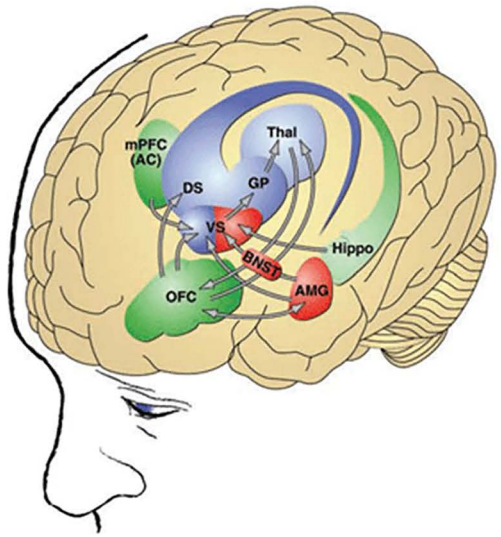

Binge/intoxication
Ventral striatum (VS), including nucleus occumbens
euphoria, reward
Dorsal striatum (DS), Global pallidus (GP), Thalamus (Thal)
habit, perseveration

Withdrawal/negative effects
amygdala (AMG), bed nucleus of the stria terminalis (BNST)
malaise, dysphoria, negative emotion states
Ventral striatum (VS)
decreased reward

Preoccupation/anticipation
Anterior cingulate (AC)
Prefrontal cortex (mPFC), orbitofrontal cortex (OFC)
subjective effects of craving, executive function
Basolateral nucleus of the amygdala
conditioned cues
Hippocampus (Hippo)
condition cues

Figure 1: Schematic of neurocircuitry for the three stages of the alcoholism cycle that drive alcohol-seeking behavior in the addicted state. VS, DS, GP and Thal activation plays a role in the binge intoxication stage. During the withdrawal-induced negative affect stage, the dopamine systems are compromised and the brain stress systems such as CRF are activated in the context of an aversive dysphoric state. The prefrontal cortex of the brain and its connections to the amygdala and the nucleus accumbens activate Glu_{ergic} neurons causing neuroexcitation. Other components in the frontal cortex are compromised, producing deficits in executive function. The compulsive alcohol-seeking behavior occurs via activation of dorsal striatal-dorsal pallidal-thalamic-cortical circuits [203] with decreased activity in the reward circuits [5].

Earlier attempts to design patient-specific treatment have failed because of lack of technology to establish alcoholism subtypes, inability to use the markers for identifying endophenotypes and a lack of diverse pharmacologic agents with proven efficacy at improving particular drinking outcomes [24-26]. Recent developments in genetic screening and transfection techniquesh as resolved some of the gaps listed above.

i. Genetic analysis may determine whether an alcohol-naive person possess the genetic vulnerabilities associated with the risk of developing alcoholism.

ii. The diagnose techniques may decipher cell-signaling abnormalities that have already occurred in alcohol abusers.

iii. It is possible to modulate the expression of selective genes by administering viral vectors containing the gene's cDNA for expression augmentation or siRNA for expression inhibition [27,28].

iv. Although these techniques may allow development of individualized therapy for alcoholism, technology to integrate all of the therapeutic components listed above is lacking. Recent development of novel Engineered Nanoparticles (ENPs) having unique electronic, physicochemical and biological properties bring hope to the development of patient-centric individual treatment of alcoholism and other addiction disorders.

ENP are < 100 nm at least in one dimension and behaves as a whole unit possessing unique electronic, physicochemical and biological properties distinct from those in bulk particles. As the ENPs become smaller, the proportion of atoms on the surface increases, thus they exhibit size- and shape-dependent properties such as electron confinement (transition from classic mechanics to quantum mechanics), metal to semi-conductor transition, an increase in mechanical adhesion and capillary forces, a drop in melting point, an increase in tunneling current, a blue shift in optical properties, and ferromagnetic to super paramagnetic shift [29]. The size-dependent unique properties of NPs are exploited by the industry to design and market new electronic, medicinal (diagnostics, prophylaxis, therapeutics and site-directed drug-transport), environmental, cosmetic, and food products that are growing every day [30]. Different ENPs are being designed and tested for screening and treatment of alcoholism and other substance addiction [31,32]. Unfortunately, the very properties responsible for ENPs' commercial application also exponentially increase their toxicity and adverse effects. As ENPs becomes smaller, its surface reactivity and toxicity increase [33,34]. The therapeutic potency/toxicity ratio may determine the therapeutic index of ENPs. Therefore, it is important to understand possible relationship between the ENPs structure and properties to develop safe and effective medicinal products including novel treatment strategies for treatment of alcoholism and development

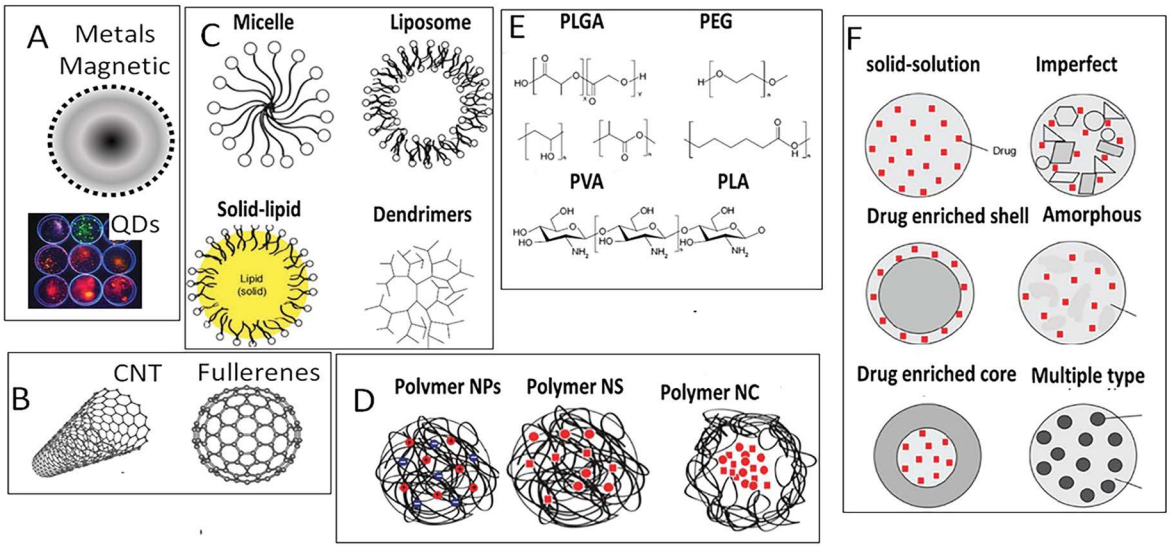

Figure 2: Schematic representations of most common types of Nanoparticles (NPs) (A) Metal, non-metal and quantum dots; (B) Carbon nanotubes and fullerenes; (C) Structure of micelle, liposomes, solid-lipid NPs and dendrimer; (D) Graphical representations of polymer NPs, polymer Nano-Spheres (NS), and polymer Nano-Capsules (NC) where charges in polymers are indicated as red and blue circles; (E) Chemical structures of the monomers; (F) Graphical representations drug incorporation in two types of polymer nanoparticles. The drugs incorporated are shown in red.

Abbreviations: PLGA: Poly(Lactic-co-Glycolic Acid); PEG: Polyethylene Glycol; PVA: Polyvinyl Alcohol; PLA: Poly-Lactic Acid; PCL: Polycaprolactone.

of personalized treatments. The aim of this review article is to discuss the ENPs' structural classification, physico-chemical properties, surface functionalization - a critical step for NP functionality, nanoparticles applications, toxicity and risk assessment and applications in alcoholism treatment.

Structure of Nanoparticles

ENPs are the simplest form of diverse structures (Figure 2) with sizes in 1 nm to 100 nm range.

According to their shape, ENPs are classified as 0, 1, 2 and 3 dimensional particles [35,36]. The '0' *Dimensional* (0D) ENPs are nanospheres and nanoclusters less than 100 nm in all dimensions (electrons are fully confined). The '1' *Dimensional* (1D) ENPs such as nanotubes, nano-rods and nano-fibers are less than 100 nm in at least two dimensions (electrons are both confined and delocalized). The '2' *Dimension* (2D) ENPs such as graphene, molybdenum disulfide and single-layer crystal composed of germanium are less than 100 nm in at least one dimensions (electrons are confined and delocalized both), while '3' *Dimensional* (3D) materials such as dispersions of nanoparticles, bundles of nanowires, and nanotubes as well as multi-nanolayers that are not confined to the nanoscale in any dimension (electrons are delocalized). Structurally, ENPs can be classified as following:

- *Metal nanoparticles* (gold, copper, silicon, iron, *etc.*) are widely used in catalysis, electronics, sensors, photonics, environmental remediation and medicine. Porous silicon nanoparticles contain microscopic reservoirs that can hold and protect sensitive drugs in a pH-sensitive manner. Acidic pH disrupts the drug-nanoparticle binding, thus releasing the drug load.
- *Polymeric nanoparticles* are prepared from synthetic polymers such as poly(2-hydroxy ethyl methacrylate), poly(N-vinyl pyrrolidone), poly(methyl methacrylate), poly(vinyl alcohol), poly(acrylic acid), polyacrylamide or natural polymers such as gums (Ex. Acacia, Guar, etc.), chitosan, gelatin and sodium alginate [29].
- *Biochemical nanoparticles* such as DNA, proteins and poly-amino acids such as poly-L-lysine and ploy-L-serine are synthesized from biological precursors. DNA nanoparticles are three strands of DNA with a lipid and functional molecule attached to its ends. In water solution, the combination of hydrophilic DNA and lipophilic lipids causes the units to self-assemble into hollow spheres consisting of multiple layers of DNA, lipid and cargo.
- *Carbon Nanotubes (CNTs)* are formed from rolling-up graphite sheets. Depending on the direction of hexagons, carbon nanotubes can exhibit metallic or semi-conductor properties. CNTs are twice as strong as steel, but weigh many times less. In 1996, a new form of carbon - the Buckminster fullerene was discovered that looks like a nanometer-sized soccer ball made from 60 carbon atoms [33,37].
- *Nanoclays* are layers of mineral silicates nanoparti-

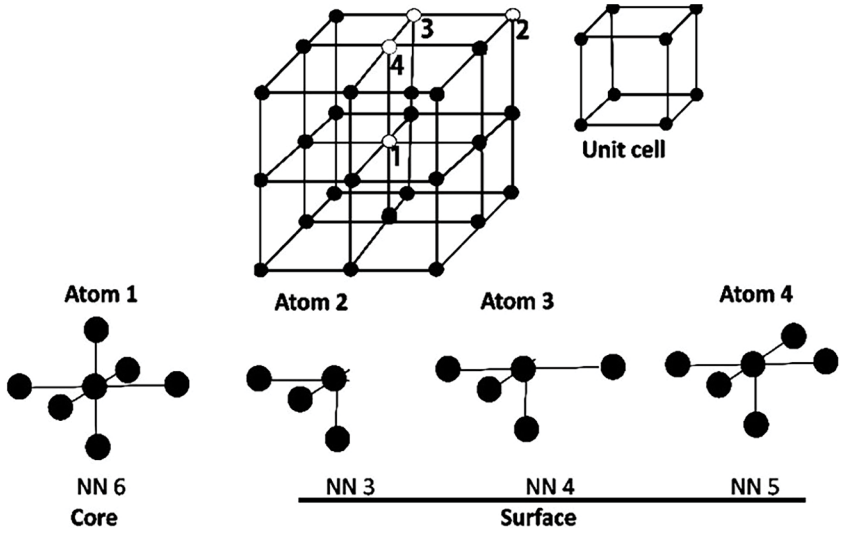

Figure 3: The 3D structure of a nanocrystal. The core atoms such as atom-1 have six Nearest Neighbors (NN = 6). The surface atoms 2, 3 and 4 have NN numbers, 3, 4 and 5, respectively. Thus, depending on the location of an atom, different surface atoms may exhibit different electronic properties, commonly known as surface anisotropy. In addition, the surface and core atoms may exhibit different electronic properties, commonly known as structural anisotropy [29].

cles. Organically-modified or hybrid organic-inorganic nanomaterials have potential uses in polymer nanocomposites, as rheological modifiers, gas absorbents and drug delivery carriers.

Physicochemical Properties of Nanoparticles

As the ENPs get smaller, there is a gradual size-dependent transition in their physical (increase in hardness, strength and ductless), optical (color change and surface Plasmon) and surface related (greater surface area to volume ratio) properties [33,38]. Below certain size (usually < 10 nm), the electronic properties of nanoparticles switch from classical mechanics to quantum mechanics [39]. The goal of this sub-sections is to discuss (i) Size-dependent properties common to all chemically diverse ENPs and (ii) Chemical-composition related distinct properties.

Common properties of all ENPs

All ENPs, irrespective of their chemistry, exhibit comparable surface reactivity, thermodynamics, and electronic and mechanical properties described below.

The surface reactivity: ENPs exhibit exceptionally high Surface Area to Volume (S/V) ratio compared to their bulk counterparts. As the ENPs' size decreases, the percentage of atoms at the surface increases relative to the core atoms, resulting in a decrease in the ENP's melting point and an increase in the (valance-conduction) band energy gap, thus many metals may become semiconductor at nanometer level [40,41]. To understand the ENP's surface effects, it is important to understand the characteristics of the core and surface atoms (Figure 3). The core atoms form stable covalent bonds with the nearest neighboring atoms. The surface atoms contain non-bonded electrons, exhibiting greater uncompensated spin. Therefore, the surface atoms exhibit relatively lower Nearest Neighbor (NN) number (Figure 3) and relatively greater free energy, anisotropy, bond defects and surface strain. These properties confer the surface atoms many unique physicochemical characteristics not present in the core atoms.

Table 1: Thermodynamic properties of bare and functionalized nanoparticles.

	PdS [176]	**CdS** [177]	**PbS** [178]	**Ag** [179]
Bulk	1.8	1.51	1.47	1.06
NP bare	6.0	2.5	2.45	6.4
NP-capped		1.74		
Embedded				1.3-5.9

Size dependent thermodynamic properties: The Gibbs free energy of bulk particles (G_b) is defined as G_b (p, T) = H - TS where H is change in enthalpy, T is temperature and S is the entropy [42]. Surface atoms have minuscule role in determining the bulk particle's G_b. In ENPs, the surface free energy begins to dominate the core free energy, thus size becomes the key determinant of their thermodynamic properties. For ENPs, $G_{surface}$ is inversely related to the Diameter (D). Table 1 shows examples of surface free energy of different nanoparticles and corresponding bulk particles. In all cases, the free energy in bulk particles was lower than that in nanoparticles. Nanoparticles capped with functional groups or embedded in another particle exhibited lower free energy. This suggests that the free surface energy of nanoparticles also depends upon their functionalization and environment (Table 1).

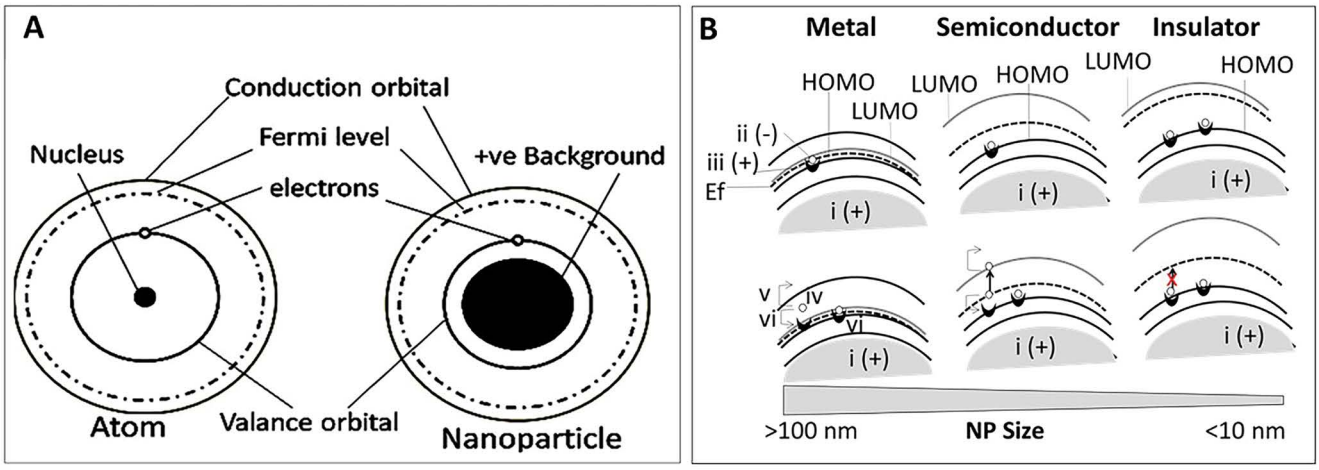

Figure 4: Electronic basis of metal to semiconductor/insulator transition of nanoparticles (A) Structure of atoms and nanoparticles. An atom consists of a nucleus (positively charged protons (4i) and neutrons) and negatively charged electrons (4ii), bound with a positron (4iii) at resting state. Electrons are distributed around the nucleus in descrete molecular orbits known as Occupied Molecular Orbital (OMO). The outermost OMO is known as the highest OMO or HOMO. The electron-positron complex, upon absorbing photons of specific wavelength, split and the acelerated electron (4iv), if possessing suffuiient energy to jump past the Fermy barrier (E_f) and if a Density of State (DOS) is available in LUMO (Lowest Unoccupied Molecular Orbitalor), enters LUMO (4v). The positron yields a net positive charge to the orbit, thus it attracts another electron from neighboring electron-hole complex (4vi). The metal nanoparticle' score is envisioned as +ve charges smeared out to a homogeneous background and only the valance and conductance electrons are treated explicitly (the Jellium structure). Therefore, an atom and a nanoparticle both may participate in chemical reactions; (B) Effects of size reduction on metal to insulator transition of a metal NP. The +ve core of the metal NP is balanced by the -ve charged valance electron in the NP's HOMO. Metals lack band gap and Eg is situated within HUMO and LUMO, thus a level of energy that splits the electron-hole complex will allow the electrons to jump from HOMO into the LUMO and leave the atom. Semiconductors have a band gap and the E_f is situated within the gap. This electron must absorb sufficient energy to split from the 'hole' and then cross the E_f to jump into the LUMO. In insulators, electrons can't absorb sufficient energy to cross from HOMO to LUMO.

Electronic properties: In bulk particles, Electrons (e^-), bound with a positively charged Electron-Hole (e^-h^+ complex), are distributed in discrete energy bands called occupied orbital's [43-45]. The number of electrons in Valance Orbital or Highest Occupied Molecular Orbital (HOMO) determines the electrical properties of an atom [46]. When an electron in HOMO is excited by absorbing energy (light or heat), it separates from the 'hole' and jump into the conduction band, resulting in creation of a positively charged 'hole' in HOMO [47,48]. The newly formed 'hole' attracts neighboring electron, resulting in propagation of a positively charged hole-current in HOMO, moving opposite to the direction of the electron current in the conduction bands [29]. In metals, since the HOMO and LUMO overlap, electrons from both HOMO and LUMO can bind the 'hole' (Figure 4).

Unlike the bulk particles, nanoparticles less than 100 nm gets quantized and acquire wave-particle duality [49,50]. Electrons are found within certain energy-states called the Density of States (DOS). Electrons cannot jump from HOMO to the Lowest Unoccupied Molecular Orbital (LUMO) if the DOS is occupied (the Pauli Exclusion Principle). The DOS of a system describes the number of states at each energy level that are available for occupation by electrons. In metals, the LUMO, HOMO and the *Fermi* level (Ef) overlap, thus electrons nearest to the Fermi level cross to the conduction band. In semi-conductors, there is an energy gap between HOMO and LUMO with the Fermi level situated in between (at 0 K, Ef = E gap/2). The electrons in HOMO must be energized to the Ef for its translocation from HOMO to LUMO. In insulators, a large band gap prevents electron transfer (Figure 4). For bulk particles, the band structure is intrinsic property of an atom that is independent of the particles' size or shape. For nanoparticles, the band structure is influenced by the particles' size and shape. The band structure in the ENPs is strongly influenced by their size and shape. Smaller nanoparticles (less than 10 nm or smaller than the electron wavelength) confine the motion of randomly moving electrons to a specific energy level (discreteness), a process known as quantum confinement. As the ENPs become smaller, a decrease in confining dimensions makes the energy levels discrete, resulting in an increase or widening up of the band-gap energy. Since the band-gap energy and wavelength are inversely related to each other, the wavelength decreases, resulting in emission of blue radiation by the nanoparticles as opposed to red radiation emitted by the bulk particles.

Optical properties: Nanoparticles, along with ex-

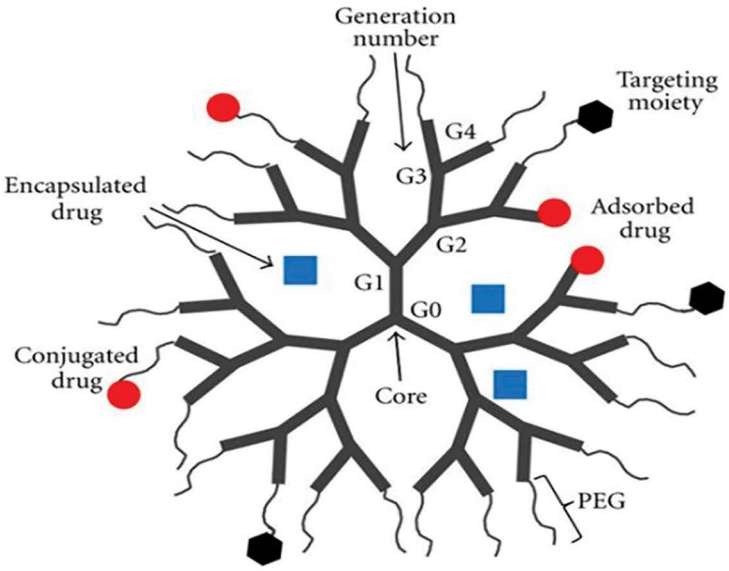

Figure 5: Structure of a functionalized G4 nanoparticle. Ab: Antibody, F2: Fluorescence probe, C: dendrimer core, G: Generation.

hibiting size-dependent increase in electronic band-gap, also exhibit a size-dependent increase in Optical Band-Gap (Og), a level of energy that activates the electron-hole complex, but is not able to free the electron for conduction [51]. The electron then returns to its original state by emitting photons in the process. The energy of the emission photon is equal to the Og energy [52]. A decrease in semiconductor particle size from bulk level (> 500 nm) to nano-level (< 10 nm) resulted in a drop in absorption from 200 nm to 450 nm [53]. Thus, as the particle size decreases, a shift in the absorption towards lower wavelengths occurs possibly because of a size-dependent increase in the Og. Absorption occurs at higher energies, resulting in a shift towards shorter wavelengths.

Mechanical properties: When the size of a nanoparticles approaches or become smaller than 10 nm, they acquire physical properties (such as friction, hardness, elastic modulus, fracture toughness, scratch resistance, fatigue strength, *etc.*) different from their bulk counterparts [54-59]. Mechanical properties may modulate the molecular forces that drive the molecular interaction, thermodynamic properties and interface of the nanoparticles with the liquid or other particles [60]. Biological systems such as proteins and DNA create interfaces with the surrounding fluids that may govern their interactions with ENPs. Interaction of cell membranes with ENPs is governed by the mechanical properties, such as friction, adhesion or elasticity, of both the cells and the materials since cells dynamically react to the mechanical cues [61]. Therefore, an understanding of the mechanical properties of ENPs is essential to bring nanomedicine from bench to clinical applications.

Particle-specific physicochemical properties

Dendrimers: Dendrimers are hyper-branched synthetic polymers that can be engineered into well-defined structures for various biological and pharmacological functions (Figure 5). Dendrimers contain a Core group (C), branching Generations (G1 to G4) and end-groups that can be functionalized with functional groups such as an Antibody (Ab) or another dendrimer containing a fluorescing group. During synthesis, as dendrimers grow in size, different generations begin to show distinct features that are amplified with increasing generations [61,62]. Some of the unique properties of dendrimers are described below.

Intrinsic viscosity (η): Intrinsic viscosity characterizes the frictional contribution of polymers in dilute solutions [63]. Dendrimers exhibit a size-dependent biphasic change in η values: the values increase as the dendrimer size increased from G0 to G4, then, further increase in the dendrimer size decreased the η values [64,65]. Unlike the η values, the hydrodynamic radius of the dendrimers increased linearly as their size increased [65].

The dendrite-box concept: The branched structure of dendrimers contains empty and defined-sized spaces surrounded by either hydrophilic or hydrophobic environment. These spaces can accept and store guest particles. The hydrophobic particles accumulate in the sites surrounded by a hydrophobic surface, while hydrophilic particles accumulate in sites surrounded by the hydrophilic environment. Once entrapped, the particles are protected from the external environment. The entrapment-space is known as the dendrimer box [66].

Biomimicry: One of the outstanding properties of dendrimers is their ability to mimic biological particles, espe-

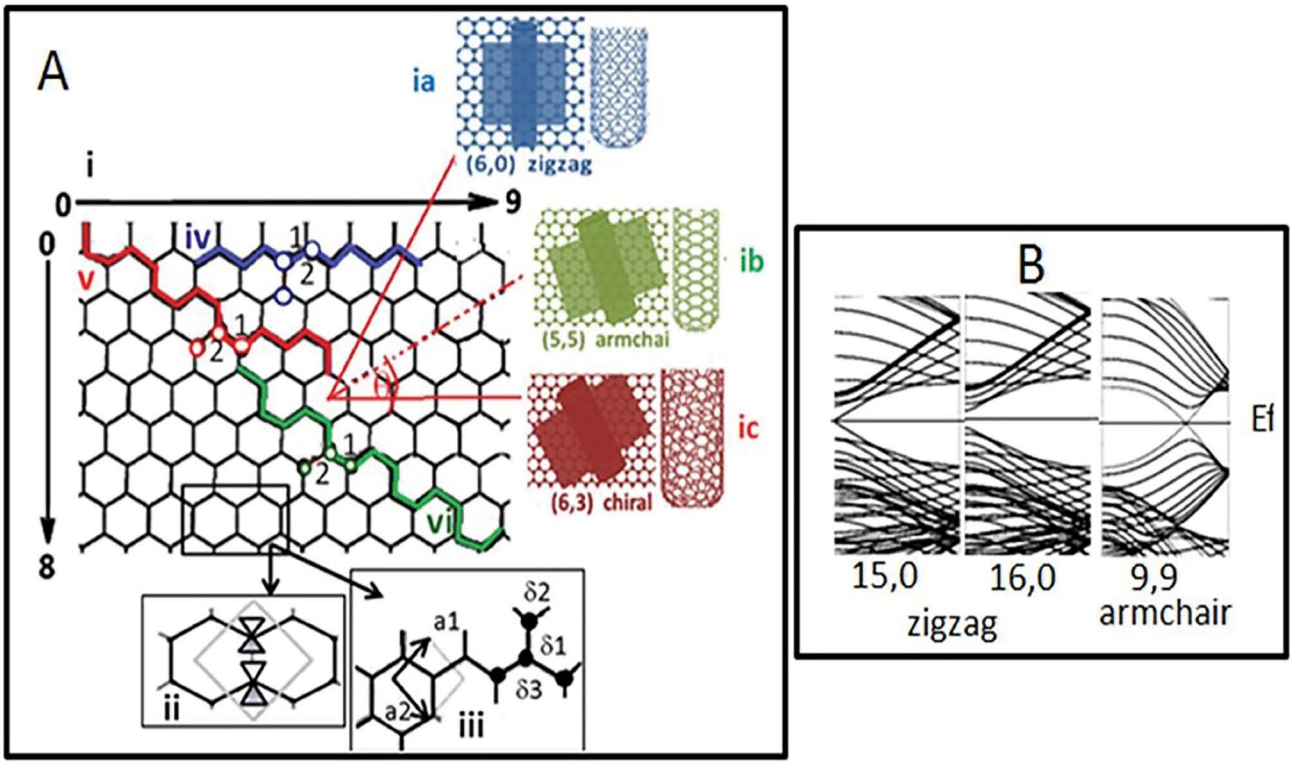

Figure 6: Structure and characteristics of graphene and CNTs. (Ai) Structure and folding of graphene sheet. The b1 and b2 bonds (1 and 2, respectively) connect neighboring atoms. Folding of graphene sheet for zigzag nanotubes shown in ia, folding of graphene sheet for chiral nanotubes is shown in ib and folding of graphene sheet for armchair nanotubes. Are shown in ic; (Aii) Graphene-unit cells containing two identical carbon atoms sharing one electron each (triangles show the density of state for each electron); (Aiii) The lattice structure of graphene is made out of two triangular lattices a1 and a2 that are the lattice unit vectors, while δ1, δ2 and δ3 are the nearest-neighbor vectors; (Aiv-vi) zigzag, armchair and chiral patterns in a graphene sheet; (B) Electronic structure (density of states) of 15,0 zigzag CNT (metallic), 16,0 CNT (semiconductor) and 9,9 armchair CNT (metallic). The (15,0) zigzag and (9,9) armchair CNTs do not have an energy gap (the HOMO and LUMO bands overlap) at the Fermi level (E_f), while (16,0) zigzag CNT has a band gap (HOMO and LUMO are separated by an energy gap) at the Fermi level.

cially globular proteins such as insulin (3G dendrimer), cytochrome (4G dendrimer), and hemoglobin (5G dendrimer) [67-70]. Dendrimers also mimic histone clusters, thus they make stable complexes with the DNA and enhance gene expression [71,72]. Like proteins, dendrimers may respond to many external stimuli and adapt a tight-packed (resembling native proteins) or extended (resembling denatured proteins) conformation [73-75].

Host-guest complex formation: The unique dendritic topology allows their application in controlled delivery agents, DNA transporters and transfection agents [62,76-78].

Properties of carbon nanotubes - metals or semiconductors: CNTs are formed by folding of a hexagonal graphene sheet consisting of unit cells [33]. Figure 6A-i shows three different patterns of graphene sheet folding, resulting in formation of three electronically different nanotubes. When n = m (like 5,5 or 6,6), the nanotubes belong to the *armchair* family (Figure 6A-ia), whereas when $n = 0$ or $m = 0$, they are called *zigzag* tubes (Figure 6A-ib). All other combinations of n and m are called chiral nanotubes (Figure 6A-ic).

The chiral angle ranges from 0° (zigzag) to 30° (armchair). The armchair CNTs exhibit metallic properties, while the zigzag and chiral CNTs can be semiconductor (containing a band gap between HOMO and LUMO) if n - m is a multiple of 3, otherwise they are metallic [79-84]. Band gaps of 0.4 to > 1 eV have been reported for SWNTs (Figure 6B).

Magnetic ENPs: Iron oxide nanoparticles, in addition to size-dependent surface characteristics, also exhibit size-dependent electron confinement and a transition from ferromagnetic (a high susceptibility to magnetization, the strength of which depends on that of the applied magnetizing field, and that may persist after removal of the applied) to super-paramagnetic (magnetization can randomly flip direction under the influence of temperature) field [85-88]. As shown in Figure 7, ferromagnetic bulk particles are multi-domain particles in which each domain's local magnetization is saturated but not parallel to other domains' local magnetization.

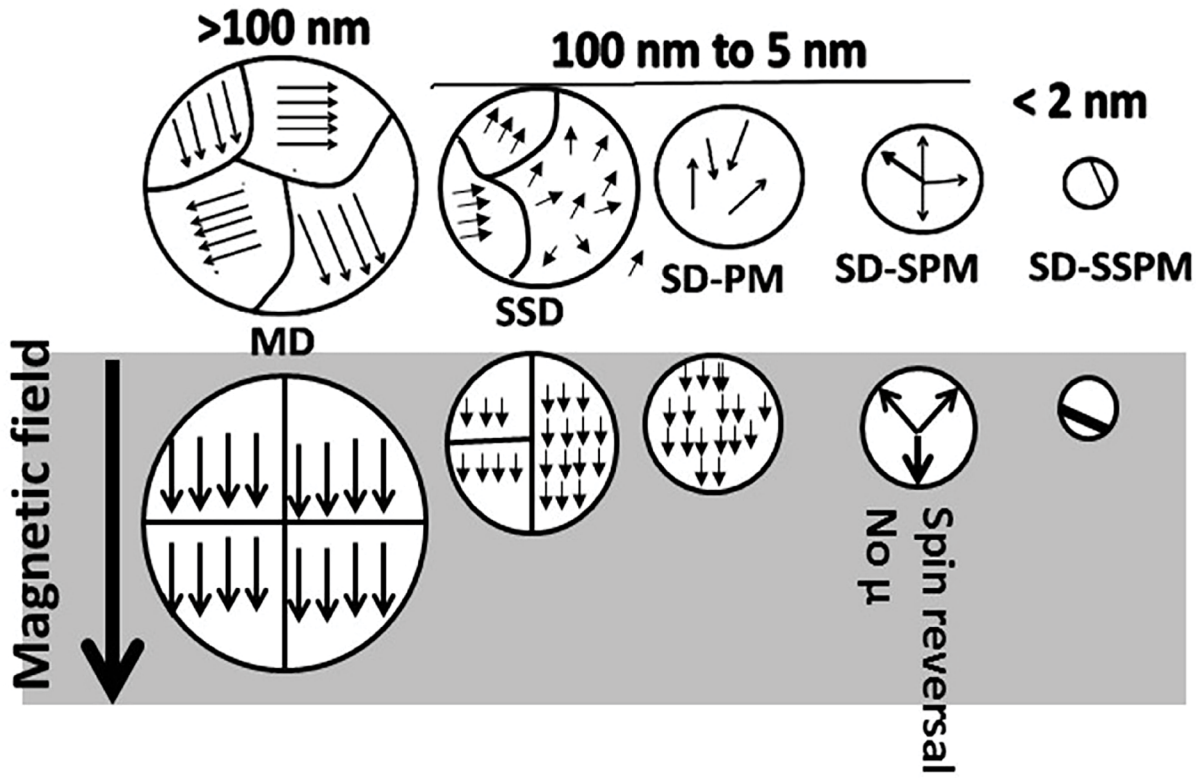

Figure 7: Size dependent alterations in nanoparticles' magnetic properties. Bulk ferromagnetic particles are Multi Domain (MD) particles. The electrons exhibit unidirectional spins in each domain, but the electrons in different domains may face in different directions. In the presence of magnetic fields, the domains (net individual electrons) rearrange such that all electrons are in the direction of the applied field. As the size decrease from 100 nm to 5 nm, it transitions into Pseudo Single-Domain (SSD), Single Domain Paramagnetic (PM) and Single Domain Super-Paramagnetic (SPM) particles, respectively. Further decrease in size transition nanoparticles in a Sub-Super-Paramagnetic Form (SSPM).

In the presence of a magnetic field, all domains exhibit parallel spin, resulting in development of magnetic field. As the particle size decreases to below 100 nm, transition from a Multi-Domain (MD) state to pseudo Single-Domain (mixture of multi-domain and single-domain properties, SSD), Single-Domain Para Magnetic (disordered atoms or electrons, SD-PM), Single-Domain Super Para Magnetic (spin reversal and loss of magnetic moment, SD-SPM), Single-Domain Sub-Super Para Magnetic (very high magnetic anisotropy showing freezing behavior, SD-SSPM) states may occur (Figure 7). The paramagnetic nanoparticles can be used in bio-imaging, while the super para magnetic nanoparticles can be used for separation processes in biochemistry.

Surface Functionalization - A Critical Step for NP Functionality

Bare (as synthesized) nanoparticles are nonfunctional because they agglomerate rapidly due to van der Waals force [89], Zeta (ζ) potential and/or the pH (close to the nanoparticles' IEP for 'zero charge') of the dispersion liquid. A ζ values greater than + 25 mV or less than - 25 mV typically indicates a stable colloid because of charge repulsion between two ENPs. Surface functionalization with diverse ligands stabilizes ENPs and confer them specific functionality (Figure 8).

Studies have shown that mono- or poly-thiol ligands such as thiolated polyethylene glycol (x-PEG-SH where x is different reactive groups for attaching a functional group such as medicine, antibody, fluorescent groups, etc.) form stronger bond with gold and silver colloid's surface, thus stabilizing the suspension [57,90-94]. Non-colloid nanoparticles can be chemically attached to Poly-L-Lysine (PLL), Poly-L-Glycone (PLG) or PEG for stabilization (Figure 7). The PEGylated ENPs, for performing specific functions, require specific end groups ($-NH_2$, -COOH, -OH, $-N_3$ and/or -SH) that interact, via either covalent or non-covalently binding, with drugs, imaging dyes, antibodies of specific proteins (Figure 9).

For achieving intracellular drug-release, acid- or enzyme-cleavable linkers that remain stable at physiological pH, but disintegrate at (i) pH less than 6.0 or (ii) in the presence of substrates, can be used [95-97]. For cancer treatment, the *cathepsin B* substrates such as Gly-Phe-Leu-Gly (GFLG) are used as the linker. Since *cathepsin B* is highly over expressed in cancer cells, the *cathepsin B* substrate-linkers are disintegrated, resulting in on-site release of drugs and/or

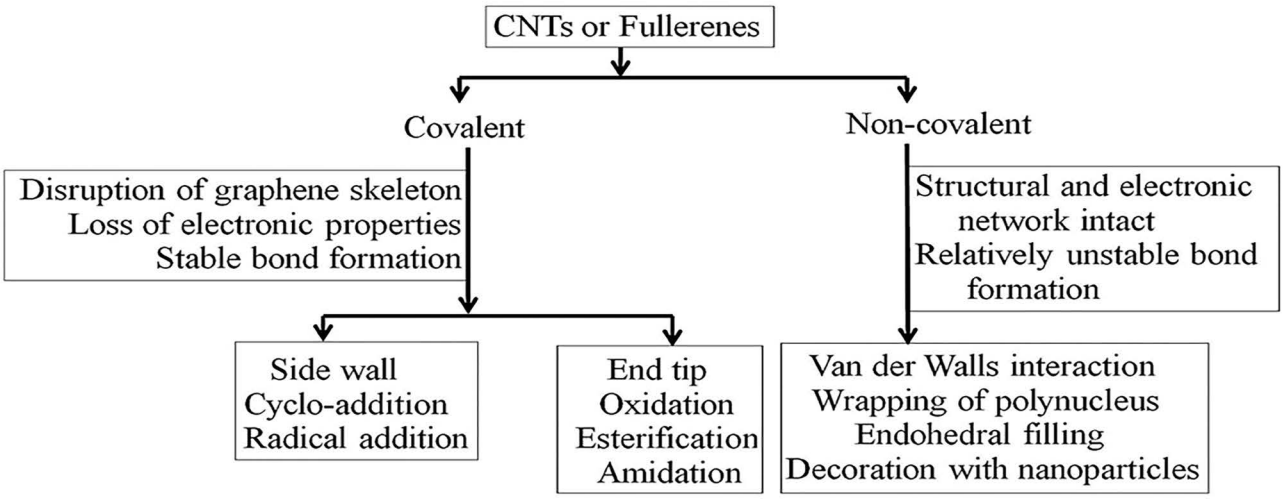

Figure 8: Overall approach for functionalization of CNTs and fullerenes.

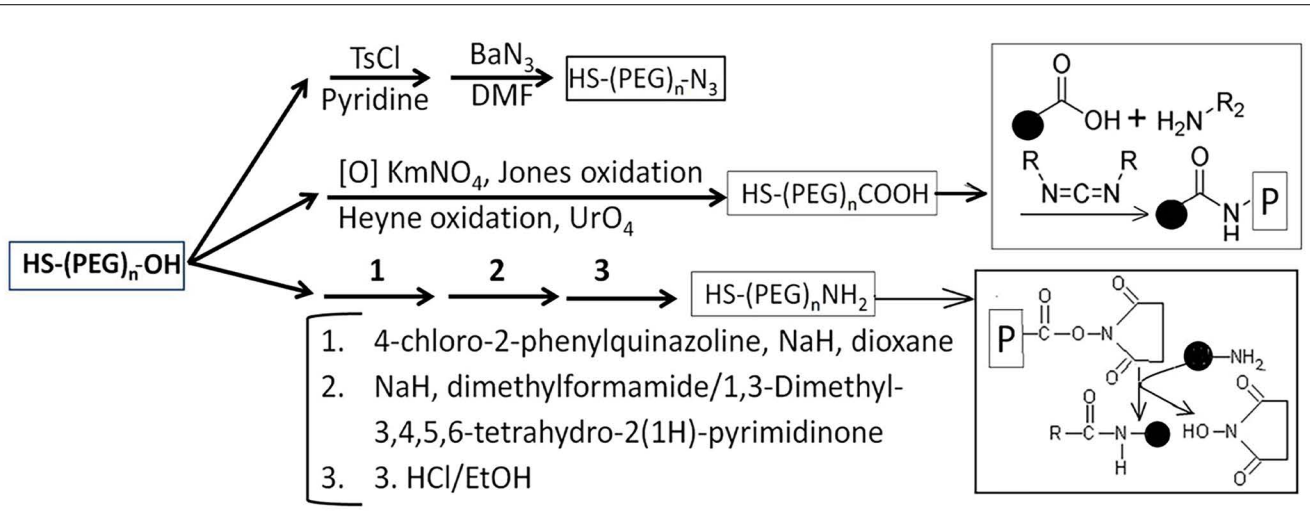

Figure 9: Conversion of hydroxyl-PEG into PEGs having other end-groups [204] Organic Chemistry Portal [205]. However, the end-groups are not highly reactive, except the -SH group that spontaneously interact with metal colloidal nanoparticles and form a stable bond [206,207]. Therefore, thiol-, amino- and carboxylic-PEGs must be activated for further reactions using agents such as maleimide, NHS ester and carbodiimide, respectively. P: protein and antibodies [208].

dyes [98,99]. Metal nanoparticles can also be functionalized with tunable switches [100] in which multiple components are not chemically bonded, but cannot dissociate because of their topological linkage. Many studies have reported DNA catenane systems with potential use in DNA topological labeling [101-104]. Functionalized nanoparticles have diverse applications described below.

Nanoparticles Applications

NPs play a central role in recent technological advances in the areas of disease diagnosis, drug design and drug delivery [105,106]. Multi-model magnetic nanoparticles contrast agents such as Super Paramagnetic Iron Oxide Nanoparticles (SPION) are anticipated to lead the way to advancements in understanding biological processes at the molecular level [107]. NPs improve efficiency of drug delivery by enhancing their bioavailability and reducing side-effects of a drug, and play an important role in development of bioassays, biosensors and biomedical devices, and bio fuel cells. Nano-chips may be a new paradigm for total chemical analysis systems [108,109]. Nanorobotics and nano-manipulation technologies will allow moving and manipulating nanoscale materials and nanoscale robotics [110]. Table 2 lists current applications of NPs in biology and medicine.

Application of nanoparticles in alcoholism treatment

Recently, nanoparticles-based therapeutic agents have acquired prominence in diagnosis and treatment of diseases including drug addiction and alcoholism, although they are not yet approved for clinical use. A review of literature provided substantial evidence for

Table 2: Lists current applications of NPs in biology and medicine.

NPs	Applications	Safety/Adverse effects	References
Gold colloid	Medical diagnostics Drug/gene delivery Pharmaceuticals	LD: Relatively safe HD: Cytotoxicity, kidney and liver damage	[180-182]
Silver colloid	Similar to Gold Antimicrobial agents Clothing odor resistance	LD: Oxidative stress HD: Neurotoxicity and liver damage, antibacterial	[183-185]
TiO_2	Antimicrobial paint, tooth paste and cosmetics	Autistic disorders, epilepsy Alzheimer's like plaques	[186-188]
Fe	Environmental remediation	Oxidative stress, inflammation liver toxicity	[189,190]
Fe_2O_3	Magnetic nanoparticle - contrast agents for tumor imaging	Oxidative stress, membrane leakage of LDH, DNA damage, inflammation	[37,191]
CNTs	Diagnostics Consumer electronics Sports equipment	Mitochondrial toxicity, cell cycle arrest, liver and lungs damage, frustrated phagocytosis	[192-195]
Fullerenes	Drug delivery	Oxidative stress, inflammation Liver damage	[196,197]
Linear polymers	Drug delivery	LD: Relatively safe HD: CNS and liver damage	[198,199]
Dendrimers	Drug delivery	Relatively safe. Some dendrimers may mimic body proteins and enzymes	[200-202]

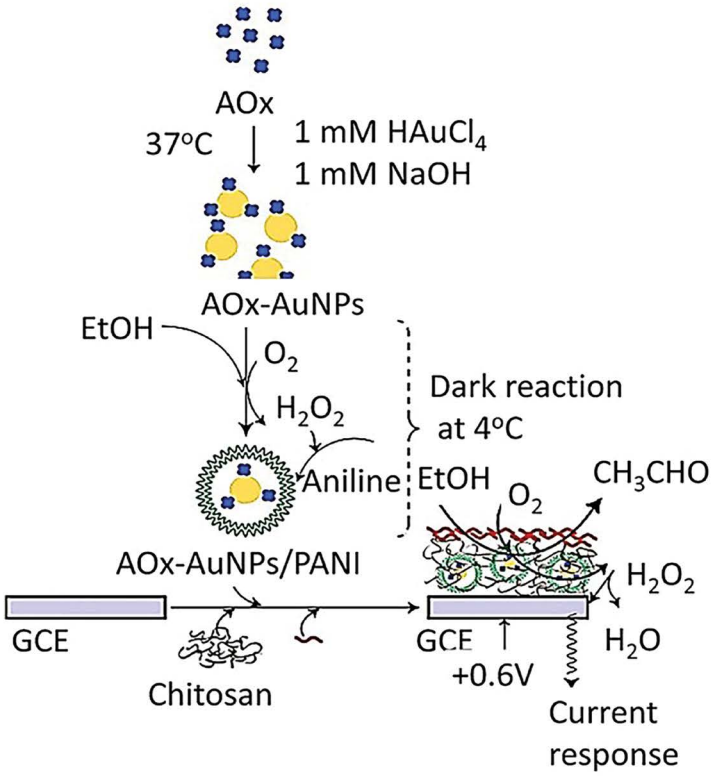

Figure 10: Diagram of a simple AOx-AuNP/PANI biosensor for sensitive detection of alcohol. The biosensor was synthesized by incubating $AuCl_4$ and AOx under alkaline condition (pH 8.5). The AuNPs-AOx conjugate was encapsulated with Polyaniline (PANI) that was stabilized on a Glassy Carbon Electrode (GCE) by chitosan-Nafion mixture. The mechanism of ethanol oxidation is shown.

Abbreviations: AOx: Alcohol Oxidase; AuNP: Gold Nanoparticles; GCE: Glassy Carbon Electrode; PANI: Polyaniline. (Adapted from Chinnadayyala, et al. [111]).

possible application of nanoparticles in diagnosis and treatment of addiction. Results from selected studies are presented below.

Alcohol Oxidase (AOx) functionalized Gold Nanoparticles (AuNPs) for development of alcohol biosensor: Chinnadayyala, et al. [111] have designed a simple AuNP-based biosensor for sensitive detection of alcohol. They synthesized AuNP using AOx protein in alkaline (pH 8.5) condition with simultaneous stabilization of the nanoparticles on the AOx protein surface. The AuNPs-AOx conjugate was encapsulated with Polyaniline (PANI) that was stabilized on a Glassy Carbon Electrode (GCE) by chitosan-nafion mixture (Figure 10). The biosensor was then utilized for detection of alcohol ampere metrically using H_2O_2 as redox indicator at +0.6 V. The fabricated bio-electrode was successfully used for the selective determination of alcohol in beverage samples (Figure 10).

Gómez-Anquela, et al. [112] used AuNPs capped with thiotic acid to coordinate with the Zn (II) present in the catalytic center of Alcohol Dehydrogenase (ADH). The complex, in combination with Azure A (the NADH oxidation molecular catalyst) was electro grafted onto carbon screen-printed electrodes (Figure 11) that were efficient ethanol biosensor. The final bio-sensing device was highly efficient in ethanol oxidation with low over potential of -0.25 V with a detection limit of 0.14 ± 0.01 μM and a stable response for more than one month. Luo, et al. [113] constructed a disposable blood alcohol biosensor prepared by immobilizing Alcohol Dehydrogenase (ADH) and Nicotinamide Adenine Dinucleotide (NADq) coated by Nafion combined with AuNPs onto the surface of Meldola's blue modified screen-printed electrodes. The sensor was capable of detecting blood alcohol concentration in laboratory medicine and forensic medicine samples.

Anti-oxidative enzyme nano-complex enhance alcohol degradation: Luo, et al. [113] constructed a robust enzyme nano-complex (Figure 12) by assembling or conjugating selected enzymes (anti-oxidative enzymes) with synergic or complementary functions in a nano-complex, followed by its encapsulation within a cross-linked polymer nanocapsule.

Exemplified by the synthesis of a triple-enzyme nanocomplex. Inhibitors for each enzyme were respectively conjugated to a single-stranded DNA with a designed sequence. Complementary assembly of the DNA molecules forms a DNA-inhibitor scaffold of a triple-enzyme nanocomplex. Subsequent *in situ* polymerization resulted in a thin layer of polymer network around each nanocomplex, and the formation of nanocapsules containing a triple-enzyme core and a permeable shell (step II). Then, removal of the DNA-inhibitor scaffolds creates a highly robust enzyme nanocomplex (step III). The nano-

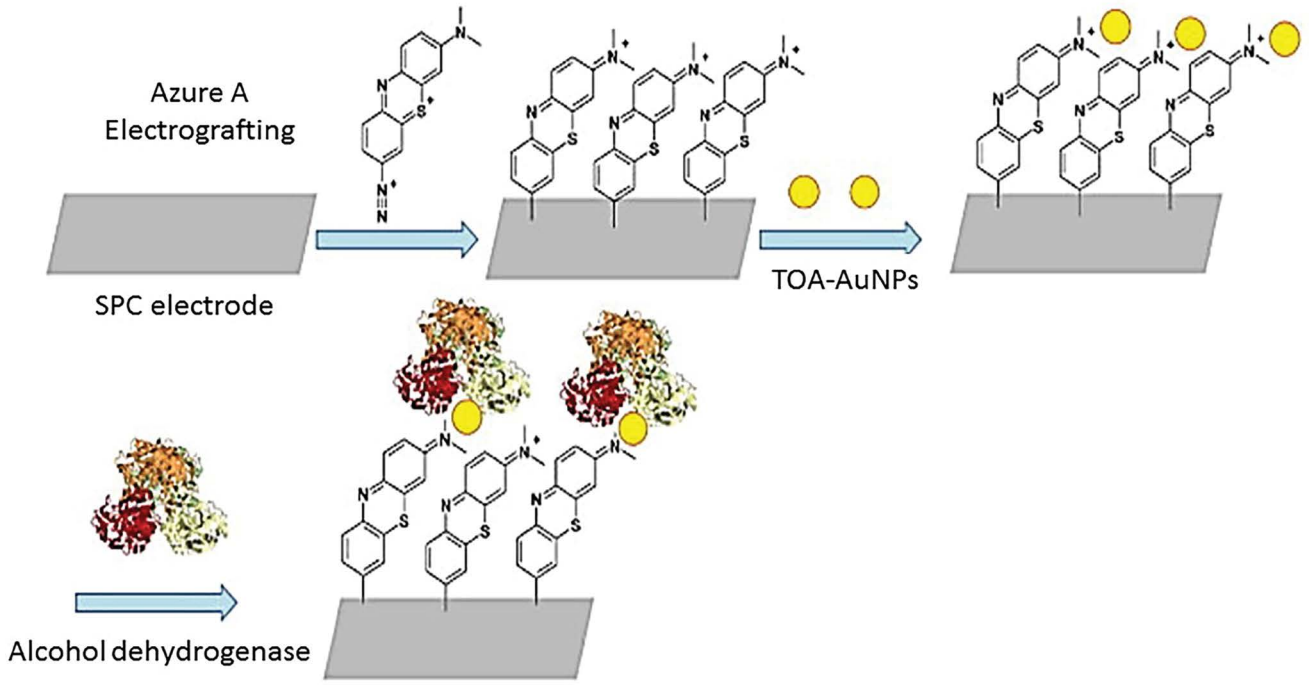

Figure 11: Diagram of the processes for development of a biosensor consisting of Azure-A annealed Scaffold Electrodes (SPCE) coupled to Thioctic Acid-Capped Gold Nanoparticles (TOA-AuNOs) and Alcohol Dehydrogenase.

Abbreviations: Azure-A: Dimethylthionine; SPCE: Integrated Screen-Printed Carbon Electrodes; TOA-AuNPs: Thiolated Gold Nanoparticles.

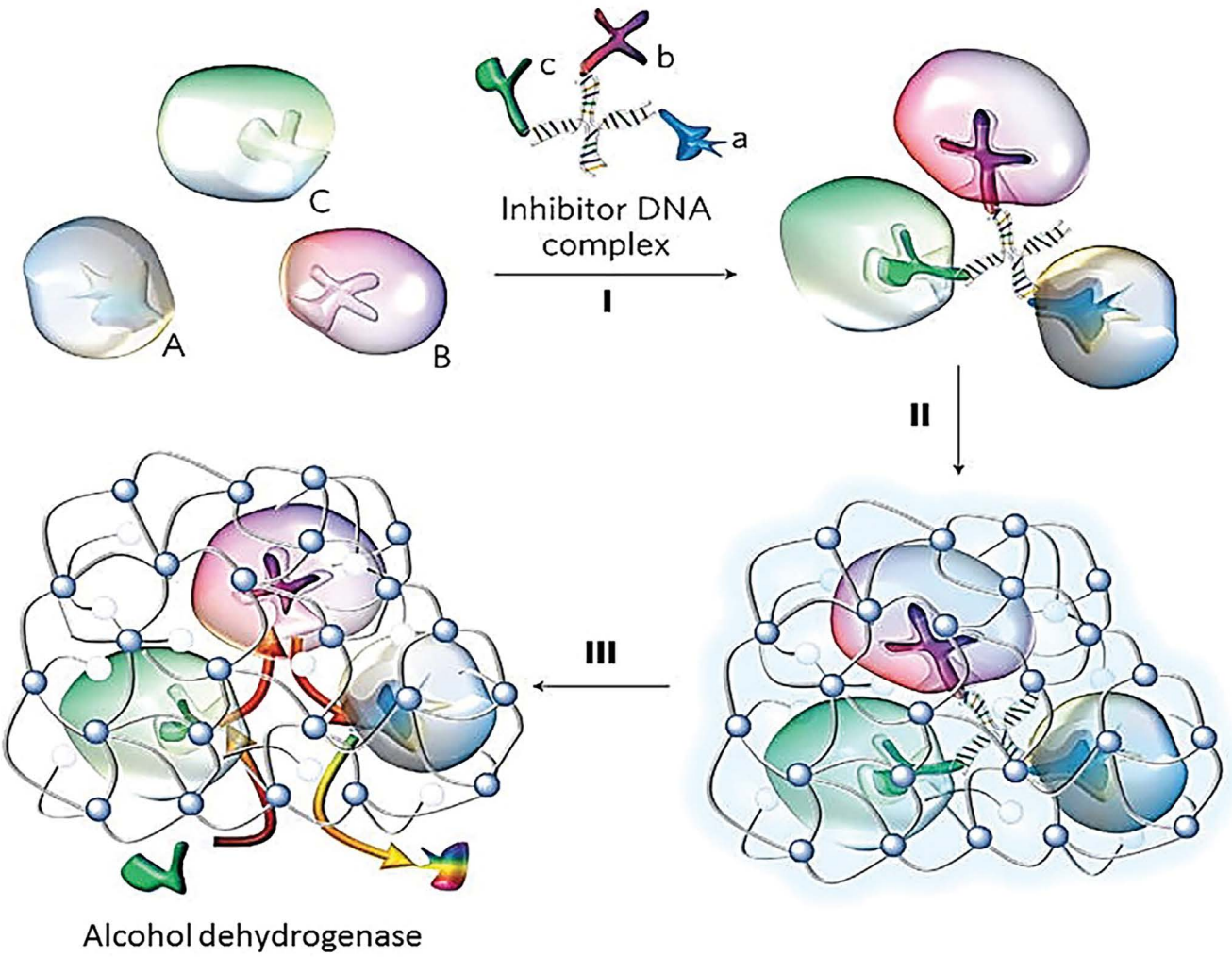

Figure 12: Diagram showing the synthesis of a triple-enzyme (Invertase) (Inv, A), Glucose Oxidase (GOx, B) and Horse Radish Peroxidase (HRP, C)) nanocomplex by DNA-directed assembly and nano-encapsulation. The enzymes were coupled with an inhibitor-DNA scaffold containing respective inhibitors, lactobionic acid for Inv (a), glucosamine for Gox (b), and 4-dimethylamino antipyrine for HRP (c) (step-I). The triple-enzyme architecture was stabilized by *in situ* growth of a thin network polymer around the enzyme nanocomplex (II). Then the DNA scaffold was removed, leading to the formation of triple-enzyme nanocomplexes that enable active transport of their reaction intermediates among the enzymes, leading to significantly enhanced reaction efficiency and complementary function, such as the capability to eliminate toxic intermediates (III). (Adapted from Liu, et al. 2013 [209]).

complexes can be further functionalized to acquire both desired surface properties and targeting capability. This study showed that the nano-complex was more effective than the mixture of enzymes for Blood Alcohol Concentration (BAC) and Alanine Amino Transferase (ALT) reduction (Figure 13). The unique n(AOx-Cat) architecture enabled effective removal of toxic H_2O_2 and prevented the AOx inactivation [114]. They showed that the H_2O_2 degradation regenerates molecular oxygen that accelerates alcohol oxidation kinetics and leading to more significant BAC reduction. Although alcohol oxidation generates another toxic intermediate, acetaldehyde, an effective ALT reduction will removal of acetaldehyde [115].

Enhancing the drug's bioavailability: Vyas, et al. [116] and Emerich, et al. [117] have shown that Nano-Functionalized Therapeutic Drugs (NFTDs) exhibited greater bioavailability than corresponding free therapeutic drugs possibly by reducing their biodegradation and/or increasing their intracellular accumulation. Yin, et al. [118] synthesized a hydrolysable cross-linked poly (ethylene glycol-graft-methyl methacrylate) di-block nano-polymer carriers for naltrexone that improved its bioavailability and site-directed release, resulting in reduced side effects. Banks, et al. [119] synthesized a nano-6-β-naltrexol, the major active metabolite of naltrexone, and administered it via a transdermal patch for treatment of alcoholism. They designed a Micro Needle (MN) skin permeation enhancement system that provid-

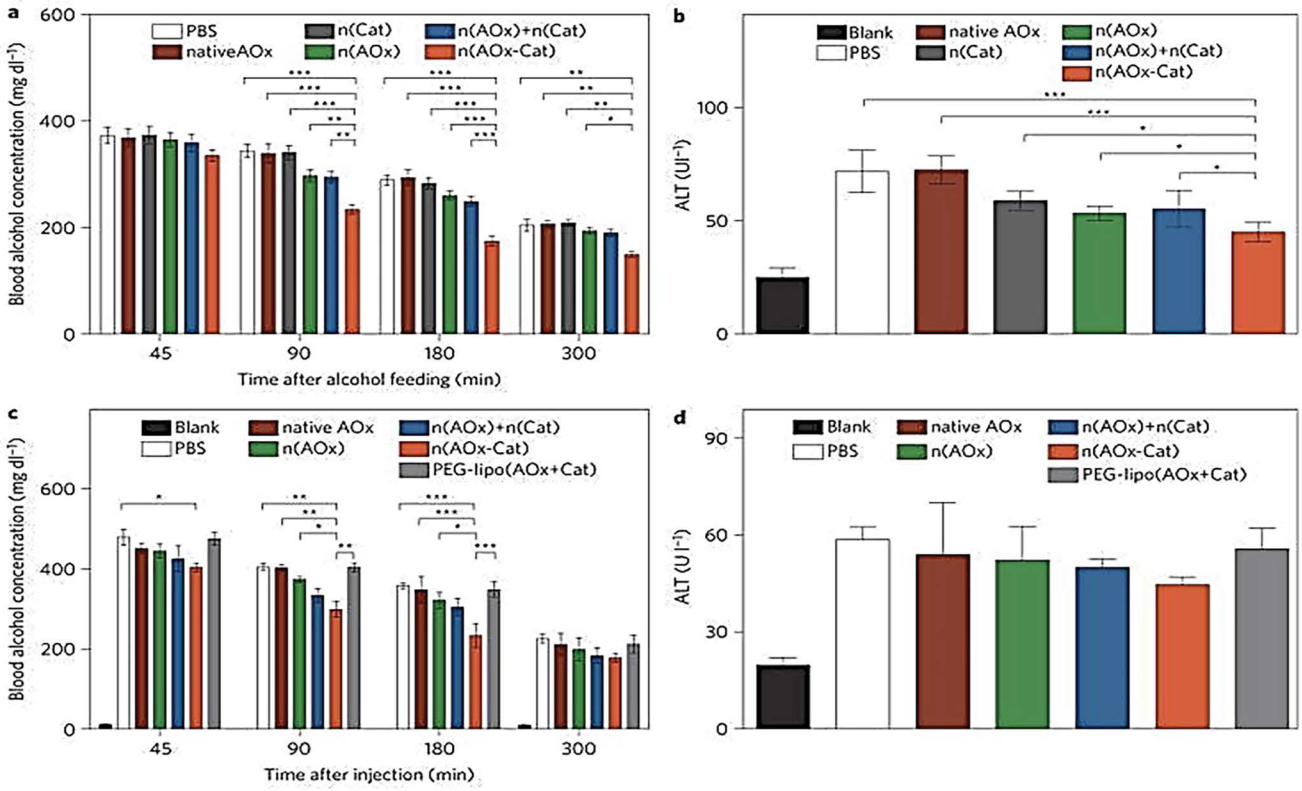

Figure 13: Efficacy of n(AOx-Cat) as a prophylactic and antidote for alcohol intoxication.

Mouse group-a and group-b: Alcohol diet mixed with the enzyme preparations (a: Blood Alcohol Levels (BAC) and b: Alanine Amino Transferase (ALT) levels in mice after gavage with an alcohol diet containing blank (no alcohol, not shown in 'a'), PBS alone, native AOx, n(Cat), n(AOx), n(AOx)+n(Cat), n(AOx-Cat)).

Mouse group-c and group-d: Alcohol diet first followed by the enzyme preparation via tail vein (c: BAC and d: ALT levels in mice gavage with an alcohol diet followed by blank (no alcohol, not shown in 'a'), PBS alone, native AOx, n(Cat), n(AOx), n(AOx)+n(Cat), n(AOx-Cat, and PEG lipo(AOx-Cat). Data are presented as mean ± standard error of the mean (s.e.m.) and the significance levels are $^{*}P < 0.05$, $^{**}P < 0.01$ and $^{***}P < 0.001$. The BAC of the mice administered with n(AOx-Cat) was reduced by 10.1%, 31.8% and 36.8%, respectively, at 45 min, 90 min and 3 h of feeding (Figure 12a). Significantly smaller BAC reductions were observed in those with n(AOx) (< 8.5%) or with a mixture of n(AOx) and n(Cat) (< 10.6%). Insignificant BAC reductions were observed for those with n(Cat) or native AOx. All alcohol-fed animals showed an increased plasma Alanine Amino Transferase (ALT) level; nevertheless, the mice treated with n(AOx-Cat) had a tendency for lower ALT levels (Figure 4b). In c and d mice also, n(AOx-Cat) is more effective than the mixture of n(AOx) and n(Cat) for BAC and ALT reduction. They show that nanocomplexes containing alcohol oxidase and catalase could reduce blood alcohol levels in intoxicated mice, offering an alternative antidote and prophylactic for alcohol intoxication. (Adapted from Liu, et al. 2013 [209]).

ed a 3.6 fold enhancement in steady state plasma concentration *in vivo*.

Engineered nanoparticles facilitate targeted delivery of therapeutic agents: Sharma, et al. [120] have shown that microinjection of Glial-Derived Neurotrophic Factor (GDNF)-conjugated nanoparticles into the rat striatum and nucleus accumbens is able to block self-administration of cocaine in rats. Green-Sadan, et al. [121] showed that transplantation of a GDNF-expressing astrocyte cell line into the striatum and nucleus accumbens attenuated cocaine-seeking behavior in Sprague-Dawley rats. Then, they developed a nano-GDNF system as a safe and effective method for introducing GDNF into the brain. An administration of GDNF-conjugated nanoparticles microinjected into the striatum and nucleus accumbens suppressed cocaine self-administration in rats. Furthermore, a cocaine dose response demonstrated that decreased lever response in rats that received GDNF-conjugated nanoparticles persisted after substitution with different cocaine doses. Carnicella, et al. [122] either an activation of the GDNF pathway or direct administration of a nano-GDNF formulation in the Ventral Tegmental Area (VTA) reduces moderate alcohol intake in a rat operant self-administration paradigm (receiving a 20% ethanol solution in an intermittent-access two-bottle choice drinking paradigm). They showed that microinjection of GDNF into the VTA 10 min before the beginning of an ethanol-drinking session.

i. Significantly reduced ethanol intake and preference, but did not affect total fluid intake and

ii. Decreased both the first bout of excessive ethanol intake at the beginning of the session, and the later intake occurring during the dark cycle.

These data suggest that GDNF-conjugated nanoparticles may serve as a novel potential treatment for drug, including alcohol, addiction. Rao, et al. [123] showed that, in addition to the GDNF, upregulation of Glutamate Transporter-1 (GLT1) by ceftriaxone (a beta-lactam antibiotic) effectively attenuated drug-seeking and drug-consumption behavior in rodent models. However, ceftriaxone treatment was not effective *in vivo* because of poor gastrointestinal absorption, serious peripheral adverse effects, and/or suboptimal CNS concentrations. They synthesized a nano-formulated GLT1 activators that selectively permeated the blood brain barrier and accumulated into the brain.

Receptor modulation by hydrated fullerenes: Tykhomyrov, et al. [124] have reported a protective effects of an aqueous solutions of hydrated C_{60} fullerenes (C_{60}HyFn) with C_{60} concentration of C_{60}HyFn on the CNS, which is above all due to its antioxidant activity, which results in the phenomenon of advanced viability of astroglial cells. On the other hand, there are some observations indicating possibilities of indirect C_{60}HyFn involvement in the metabolism of some neurotransmitters. In particular, it has been previously shown that C_{60}HyFn manifest positive influence on adrenergic, $GABA_{ergic}$, histaminergic and especially on serotoninergic systems that improve adaption capacity of organism to the action of various deleterious factors (http://fullwater.com.ua) [125]. Taking into consideration the wide range of biological activity of hydrated fullerene both at molecular and physiological levels, absence of any toxicity, and effectiveness even in super-small doses, aqueous solutions of C_{60}HyFn can be proposed as reliever of CNS dysfunctions induced by alcohol consumption and continual alcoholization.

Gold nanoparticles synthesized by plant-extract attenuate alcohol drinking and withdrawal symptoms in alcohol preferring rats: AuNPs are commonly synthesized using the traditional reduction of chloroauric acid ($H[AuCl_4]$) by reducing agent $NaBH_4$, N_2H_2, NH_2OH or $(CH_3)_2NH{\cdot}BH_3$ [126,127] that required dispersants (such as polyethylene glycol) to prevent aggregation and complex surface functionalization for desired biological activity. Recent studies have proposed an alternative reduction method using plant extracts and gum for synthesis of AuNPs [128-134]. This process is also known as 'green chemistry for synthesis of nanoparticles' in which reactions occur at ambient temperatures (high temperatures may yield uniform size particles), neutral pH, low costs and environmentally friendly fashion [131]. AuNPs synthesized using plant extracts demonstrated procedure-dependent variations in size (Figure 14), low protein adsorption (low corona formation), poor aggregation into larger particles, and higher sta-

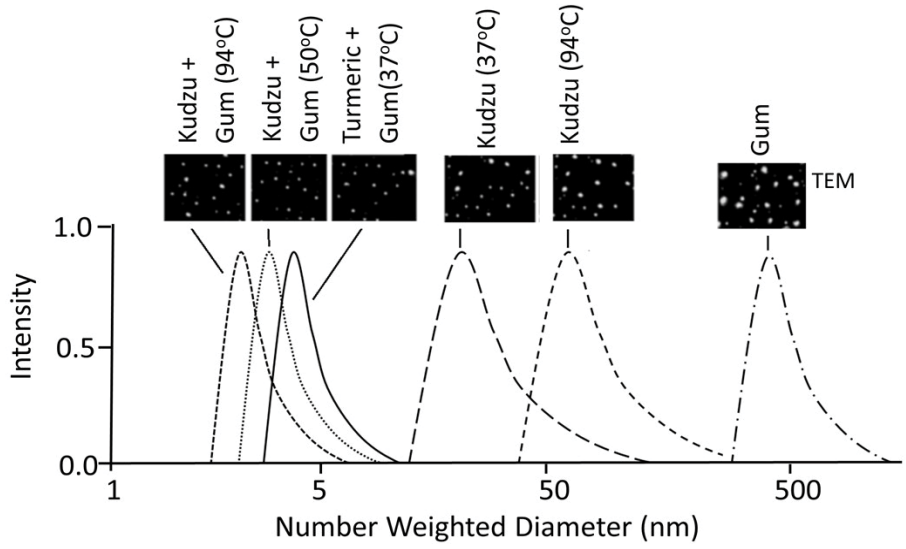

Figure 14: UV-Vis spectrum and TEM (Hitachi model HF-2000 field emission transmission electron microscope) of gold nanoparticles synthesized using different plant extracts (kudzu root extract (aqueous) + gum Arabic solution at 94 °C, 50 °C and 37 incubation (for 4 h) temperature, Kudzu extract alone at 94 and 37, and gum alone at 94). The UV-Vis spectrum (Varian FTS 1000 FT-IR Spectrometer) was measured at exciton band near 550 nm to assess particle formation. After predetermined time, the mixture was centrifuged and the AuNP pellets were collected and washed 3x with distilled water. The TEM (Hitachi model HF-2000 field emission transmission electron microscope with a resolution of 0.1 nm) analysis was performed as described previously [135]. This study showed that a mixture of kudzu extract and gum yielded smaller AuNPs (3 nm to 20 nm diameter). Kudzu alone yielded particles ranging from 20 nm to 350 nm and gum alone yielded much larger particles. The TEM images confirm that larger particles are not due to aggregation of smaller particles (Singh, 2017 [210] unpublished data).

bility at physiological condition compared to chemical reduction and citrate capped nanoparticles [128]. AuNP size can be controlled by controlling temperature and/or the incubation composition.

A recent study from our laboratory (unpublished data) compared the effects of four AuNP preparations (KG@AuNP synthesized by kudzu extract and plant gum (7 to 10 mn, Figure 10), K@AuNP synthesized by kudzu extract alone, K + G + $AuNP_{PEG}$ that is a mixture composed of traditionally synthesized AuNP stabilized by PEG, kudzu extract and gum solution and $AuNP_{PEG}$ alone) on alcohol preference [(alcohol intake/total fluid intake) × 100] and the severity of the withdrawal symptoms in alcohol preferring rats. As shown in Figure 15, KG@AuNP administered rats exhibited smallest alcohol preference than K@AuNP, K + G + $AuNP_{PEG}$ or $AuNP_{PEG}$ administered rats allowed to self-administer alcohol as described previously [135]. In addition, the severity of the withdrawal symptoms showed the following patterns: KG@AuNP rats < K@AuNP rats < K + G + $AuNP_{PEG}$ < $AuNP_{PEG}$ rats. These preliminary observations suggest that KG@AuNP (AuNP synthesized by kudzu extract and plant gum solution) protected against, while the traditionally synthesized $AuNP_{PEG}$ augmented the adverse effects of ethanol drinking in alcohol preferring rats. This suggests that the plant-extract synthesized AuNPs may have therapeutic potential against development of addiction in humans (Figure 15).

Smart, multifunctional nanoparticles: As discussed above, alcoholism is complex, progressive, multifaceted disorder that cannot be efficiently treated with current therapeutic approaches. Although simple functionalized ENPs, described above, provide a unique approach in addiction treatment, they lack capacity to release cargo (TDs, siRNAs and/or plasmids inserted with specific cDNAs) in spatial-, temporal- and dosage-controlled fashions, on demand. Recent progress in nanotechnology and material chemistry has allowed construction of

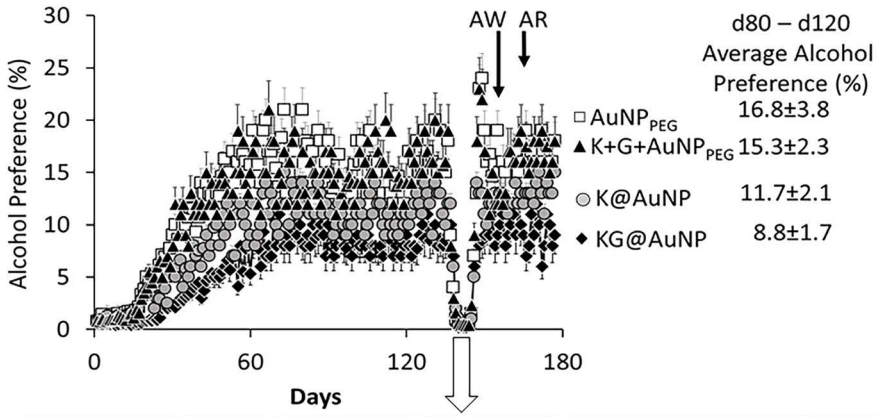

	Control	Alcohol (A)	A + AuNP-PEG	A + Kudzu@AuNP	Kudzu extract
Sensitive to touch	none	4 (n=8) 2(n=2)	4 (n=10)	2 (n=6), none (n=4)	1 (n=4)
Landing Abnormality	none	3 (n=10)	3 (n=10)	2 (n=6), none (n=4)	2 (n=4)
Tremors	none	3 (n=6)	none	none	none
Seizures	none	none	none	none	none

Figure 15: Effects of plant-extract synthesized AuNPs on alcohol abnormalities in Alcohol-Preferring (AP) rats. The AP rats (males, 100 g to 150 g) were allowed to self-administer 8% ethanol solution using (one bottle contained ethanol and the other pure water) a procedure described earlier [135]. Rats were divided into 5 groups and gavage PBS (group-1), $AuNP_{PEG}$ (synthesized as described by Singh, et al. (2013) [135]) solution -20 mg/kg (group-2), a mixture consisting of $AuNP_{PEG}$, kudzu extract - Puerarin (PU) adjusted to 150 mg/kg and gum solution - adjusted to 10 mg/kg (group-3), K@AuNP synthesized using kudzu extract alone -20 mg/kg (group-4) and KG@AuNP synthesized using kudzu extract and gum -20 mg/kg (group-5). Water and alcohol intake was monitored daily when the samples were replaced. Alcohol was withdrawal at day-120 and resumed again at day-126. Rats were monitored for the development of the withdrawal symptoms as described by Benlhabib, et al. [211,212] and listed in this figure. This study showed that the PBS fed rats exhibited approximately 14% alcohol preference that did not differ significantly from the rats receiving $AuNP_{PEG}$ or $AuNP_{PEG}$ + kudzu + gum. Alcohol preference decreased slightly in rats receiving K@AuNP and decreased significantly in rats receiving KG@AuNP. Rats receiving PBS, $AuNP_{PEG}$, and $AuNO_{PEG}$ + kudzu + gum exhibited comparable severity of the withdrawal symptoms, except seizures. The severity were considerably lower in the rats receiving KG@AuNP. This suggests that the plant-synthesized AuNPs retained the medicinal properties of the extract.

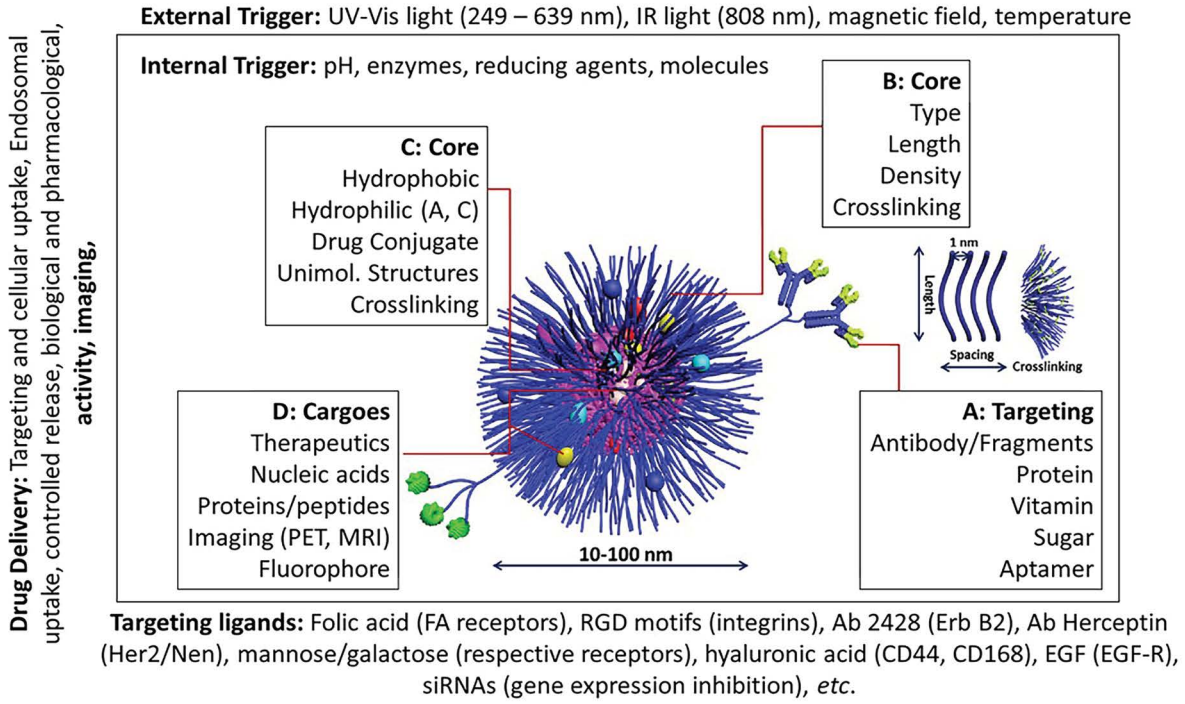

Figure 16: Composition of 'smart' multifunctional nanoparticles for therapeutic, biomedical delivery and imaging applications. (A) Core: nature of the (core hydrophobic, hydrophilic, polymeric, metal, magnetic or QD) dictates the overall function of the NPs and type of the drug to be encapsulated. Magnetic NPs and QD core may facilitate imaging, while polymeric dendrimers may facilitate development of multifunctional NPs; (B) Functionalization: The surface is functionalized with a variety of ligands to enhance stability, prevent aggregation and corona formation, or attach functional groups; (C) Clusters of targeting moieties allow multivalent binding to receptors for enhanced cellular uptake. The use of various ligands (antibody, antibody fragment, peptides) allow specific binding of the ligands to a receptor, ion channel or enzymes; (D) Cargo: Nanoparticles can be loaded with a wide range of therapeutics ranging from small molecules to macromolecular cargoes in various ways: covalently bound to a ligand such as PEG that interacts with the core, filled in a dendrimer's hydrophilic or hydrophobic space, and cargo releasable via an internal or external triggers for on-demand release.

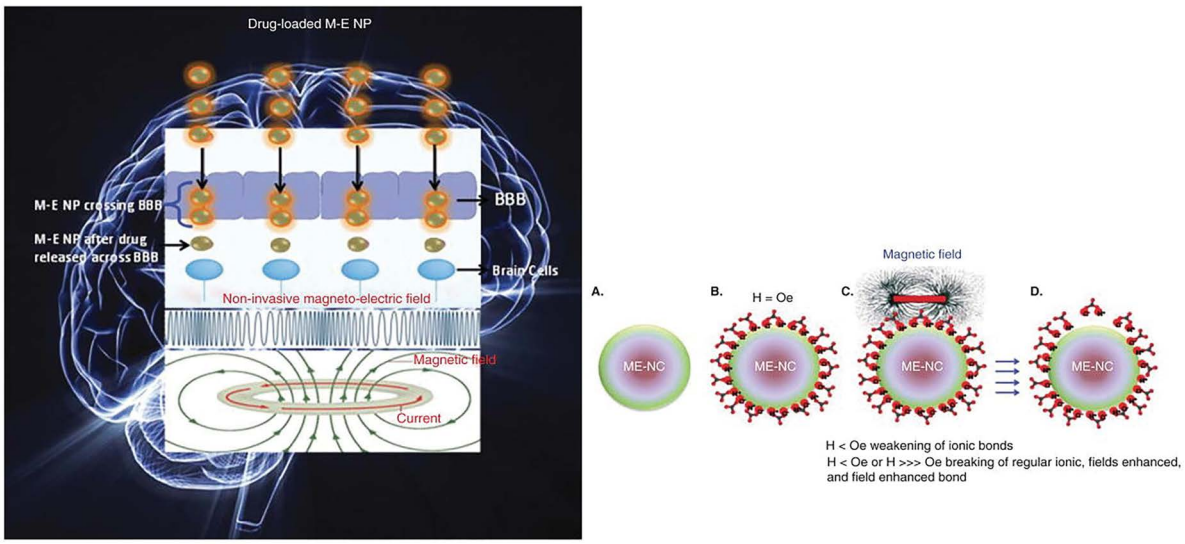

Figure 17: (i) Schematic representation of drug loading onto Magneto-Electric Nano-Carriers (ME-NCs) and on-demand-controlled drug release under the influence of external magnetic field. Surface functionalized super paramagnetic ME-NCs (A) binds with drug (or other ligands) via electrostatic interaction (B). On-demand drug release by ME-NP stimulated by a uniform alternate current magnetic field (C and D). (ii) Proposed schematic of ME-NCs-based ARV drugs delivery across the BBB (ARV: Anti-Retro Viral; BBB: Blood-Brain Barriers; ME-NC: Magneto-Electric Nano-Carriers). Nair, et al. [213] proposed that in an alternate current magnetic field, all bonds between drug and ME-NCs formulation breaks uniformly and efficiently, result in a rapid release of the cargo [214].

'smart' stimuli-driven devices that can (i) Simultaneously provide imaging, stimulation and drug delivery and (ii) Deliver the uploaded cargo on demand in selected regions and doseregime (Figure 16). The stimuli-driven NPs respond to various internal and external stimuli listed in Figure 15. The targeted release of the loaded materials to a specific site (such as a brain region) can be magnetically guided by using magnetic nanoparticles (Figure 17) [136,137]. Timed-release can be achieved using light or ultrasound cue [138]. Further research is needed to design and validate 'smart' nanoparticles for alcoholism treatment (Figure 16 and Figure 17).

Nanoparticle Toxicity

As discussed earlier, a decrease in nanoparticle size is associated with an increase in the percentage of atoms at the surface of a given material (Figure 18), leading to an increase in surface activity and acquisition of novel properties not found in bulk properties.

These unique traits of NPs are being appealed for biomedical purposes. Unfortunately, the very unique properties also enhance their intrinsic toxicity as compared to their bulk counter parts [139]. Currently, diverse groups of pure and hybrid nanoparticles are being incorporated in household and medical products. Thus, analysis and characterization of a multitude of new materials present a real challenge, but essential to assure their safety to general public. Although numerous animal studies have evaluated the toxicity of ENPs, they did not consider appropriate particle characterization, cellular uptake mechanisms, relevant doses matrices and exposure duration [140-142]. The aim of this section is to characterize toxicity of ENPs relative to those of bulk particles.

Toxicity principles

In general, there are three basic Toxicology Principles (TP) designed for bulk particles:

1. *The dose (mass-based) makes the poison* (Paracelsus theory). In general, dose is defined as the mass of a chemical per unit of body weight such as g/kg body weight. From Paracelsus's time to the present, the mass-based dose has been used to determine a chemical's beneficial effects and toxicity. The mass based dose-response relationship is the key determinant of a chemical's toxicity and the risk it poses to humans and animals.

2. *The biological actions of a chemical are specific to the chemical's structure*. In 16th century, Ambriose Paré recognized that each chemical may exhibit unique toxicity related to its structure.

3. *Humans are animals*. Therefore, protection against the toxicity of agents would be impossible without the ability to study the effect of toxins in laboratory animals.

Nanoparticles defy the 1st principle, that is *the mass-based dose makes the poison* [143-146], since dose in terms of size (diameter/kg), surface area/kg or particle number/kg is, if not more then, at least, as important as the mass-dose in correlating with toxicity [147]. This is because surface molecules, not the core molecules, determining the ENPs' physicochemical, biological and adverse properties. As an example, for equal mass of 5 nm, 10 nm and 100 nm AuNPs, the particle enumeration, surface area, surface activity may increase with a decrease in their size (5 nm > 10 nm > 100 nm. Since the biomedical and toxicological properties of ENPs are dependent on their size and/or surface properties, their toxicity may increase with a decrease in size or an increase in particle enumeration (Figure 19).

The plots of mass-dose against toxicity, shown in Figure 20, revealed that different sized nanoparticles

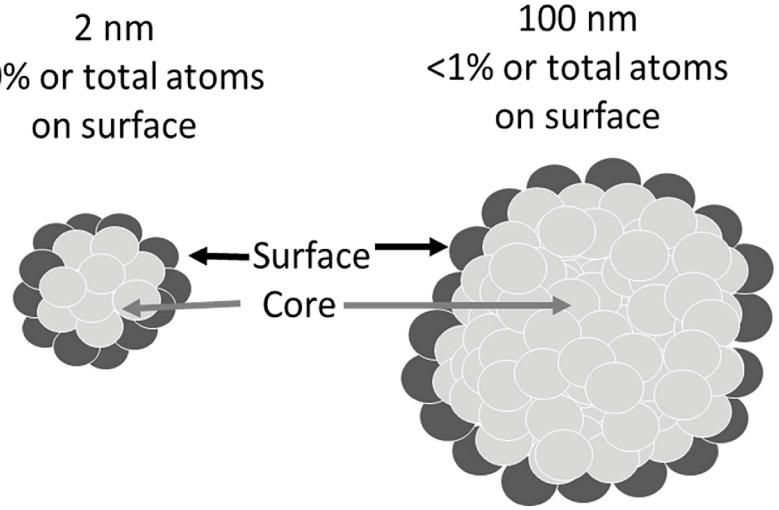

Figure 18: Surface atoms in relation to core atoms for nanoparticles and bulk particles.

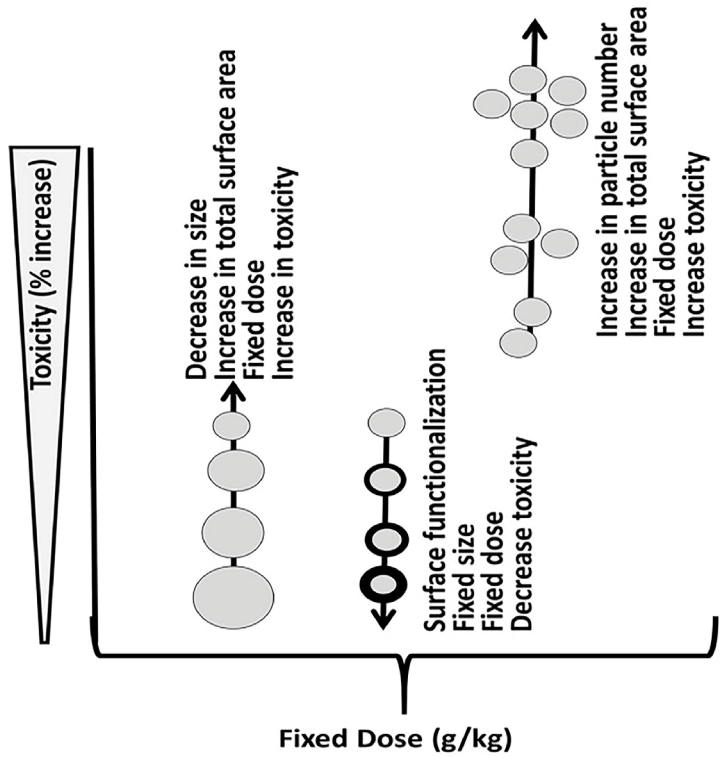

Figure 19: Size and surface-dependent toxicity of nanoparticles. At a fixed dose, toxicity of a nanoparticle is inversely related to the size and directly related to the particle number. Surface functionalization may decreases nanoparticle toxicity.

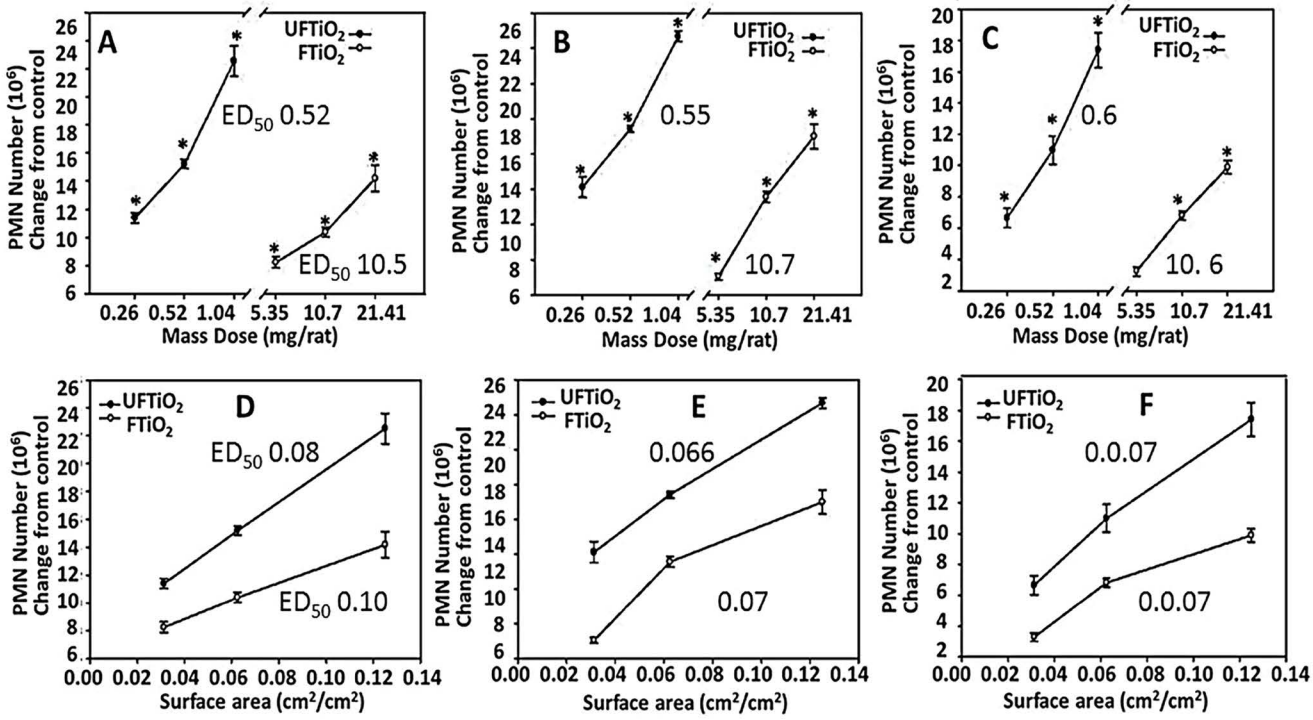

Figure 20: Nanoparticle dose (in terms of mass and surface area) and response curves for nanoparticle toxicity. Rats and mice were instilled with ultrafine (20 nm) and fine (250 nm) TiO_2 via their intra-tracheal instillation of (i) different mass doses (A, C) and (ii) different surface area dose (B, D). The Percentage of neutrophils in lung lavage of rats (A, B) and mice (C, D) at 24 hr after intratracheal instillation was used as indicators of inflammation. The 20 nm TiO_2 exhibited steeper dose response than 250 nm TiO_2 when the dose is expressed as mass (A, C). The two nanoparticles exhibited same dose response relationship with dose expressed as particle surface area (B, D). This indicates that particle surface area seems to be a more appropriate dose metric for comparing effects of different-sized particles having the same chemical structure (anatase TiO_2 in this case). Data show mean ± SD. (Adapted from Oberdörster, et al. [215]).

yielded different slopes and ED_{50} values. Thus, the mass-based dose response curve may not accurately describe the ENP toxicity, a departure from bulk particle toxicity that strictly follows the classic mass-based dose dependence. Many studies have shown that the dose as particle number, surface area (nm^2), surface to volume ratio and/or surface reactivity may characterize the toxicity of nanoparticles [142,148-150]. Thus, diameter-response, surface area-response and/or enumeration-response relationships may be important in determination of the ENPs' toxicity that can be used for risk assessment. The surface area is a better index than particle enumeration or mass in determining the inflammatory effects of nanoparticles (Figure 20) [143,151,152].

An important, but least studied, aspect of ENP toxicity is formation of protein corona. ENPs, when in contact with biological fluids, adsorb diverse type of biomolecules (*e.g.*, proteins) called protein corona that dictates the ENPs interactions with the biological systems and ensuing biological fate, therapeutic efficiency and toxicity (Figure 21) [153].

Rapid corona formation is found to affect hemolysis, thrombocyte activation, nanoparticles uptake and endothelial cell death at an early exposure time [154]. In general, there are two types of corona: initially soft (reversible binding) followed by hard (irreversible binding and structure change) corona [155]. During soft corona phase, the physicochemical characteristics of corona may change spatially and temporally, resulting in highly heterogeneous population of ENP that may alter the particle's properties and toxicity. The gold and silver

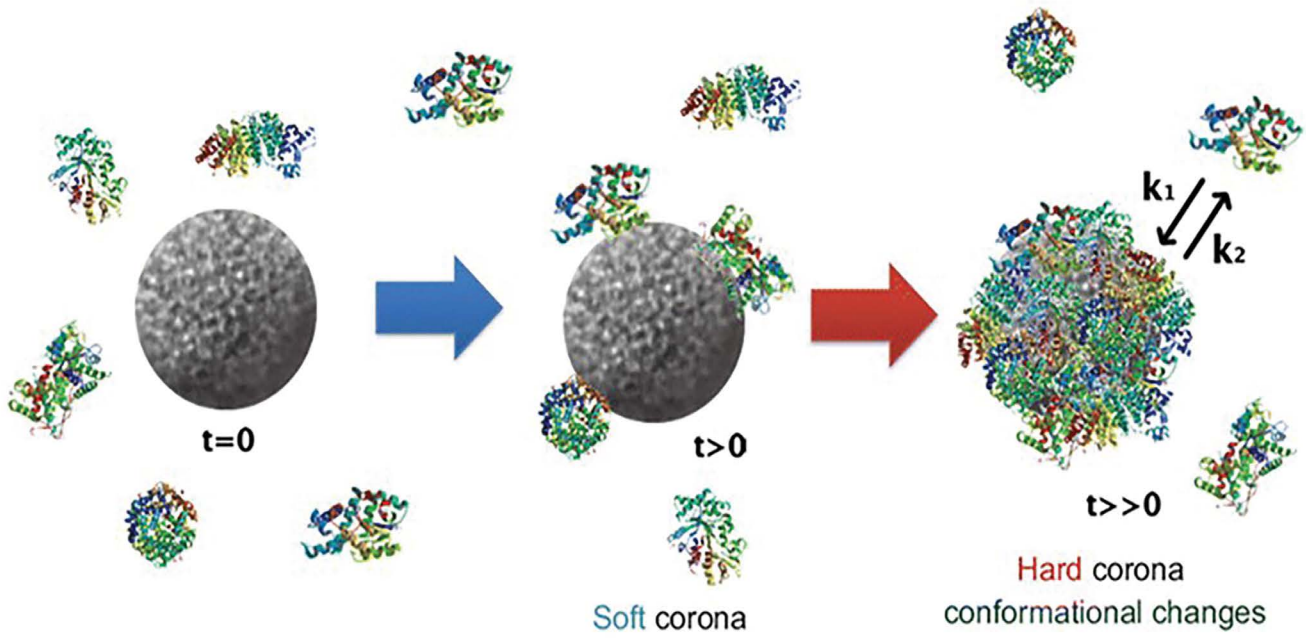

Corona	Soft	Hard
K_d (dissociation constant)[9,20,54]	High	Low
Adhesion to hydrophobicity[35]	Low	High
Molecular weight[25,32]	Low	High
Endosome–Lysosome trafficking[13,21]	Low*	Low*, High†
Conformational changes (sheet)[35,43]	Low	High

Figure 21: Schematic illustration and characteristics of a hard and a soft protein corona encompassing the nanoparticles. Hard coronas exhibit high affinity and slow exchange (i.e., several hours) and lower abundance of proteins, whereas soft coronas exhibit low affinity but rapid exchange (i.e., several minutes) of proteins. There is a different response of cellular and biochemical factors by soft and hard corona formation.

*Compared with serum-free condition; †Compared with soft corona. (Adapted from Lee, et al. [161]).

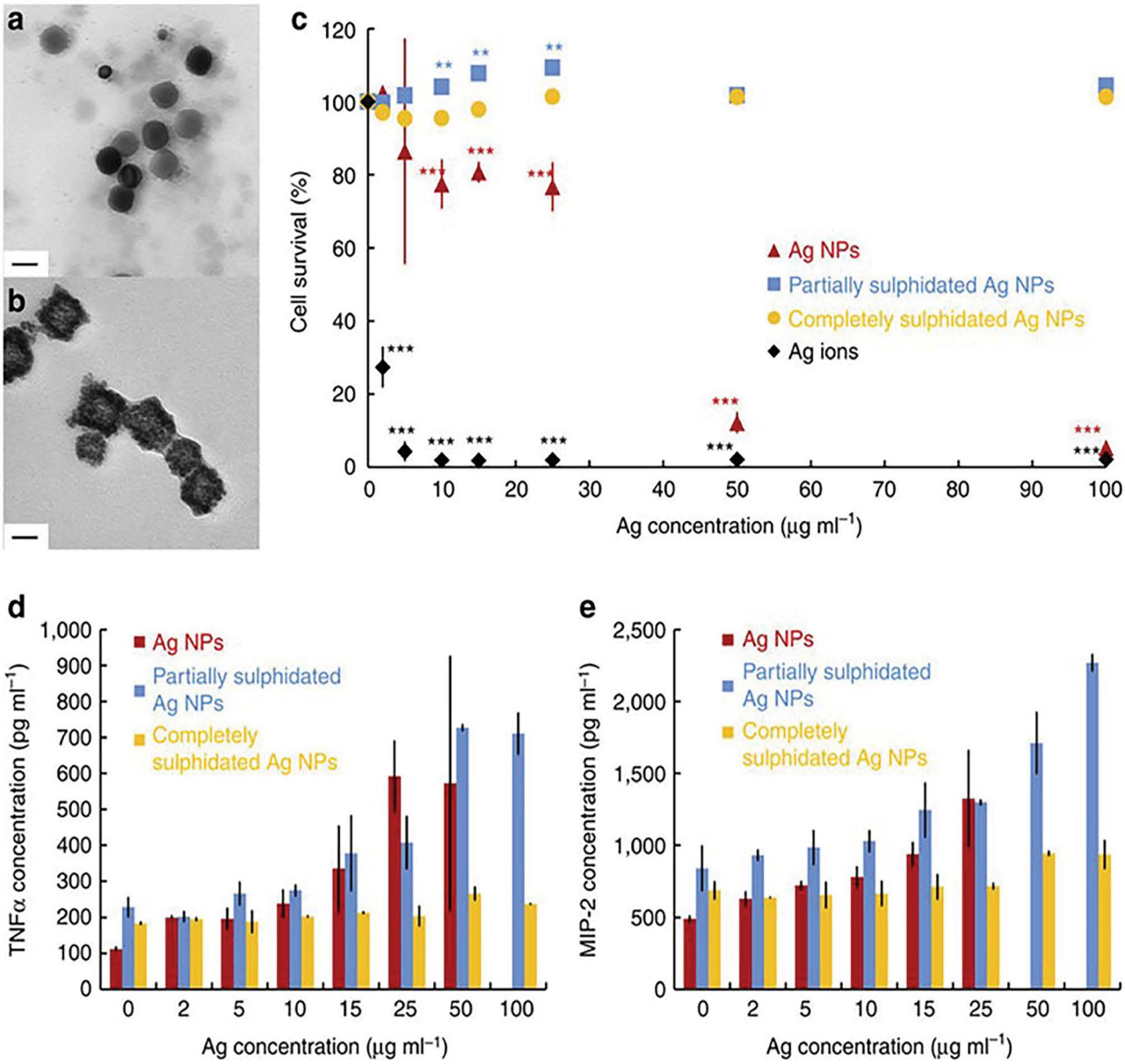

Figure 22: Protein affinity of partially and completely sulphidated silver nanoparticles. Partially sulphidated and completely sulphidated AgNPs were pre-incubation in RPMI-1640 with 10% FBS. The TEM images (a-partially sulphidated, b-fully sulphidated) were captured and viability of J774 murine macrophages was measured (c) with MTT assays after 24 h exposure to various concentrations (2, 5, 10, 15, 25, 50 and 100 µgml^{-1}) of Ag^+ ions (black diamond's), pristine Ag NPs (red triangles), partially sulphidated Ag NPs (blue squares) and completely sulphidated Ag NPs (orange circles). Error bars are provided as standard deviation; statistically significant differences as compared with the control are marked ($^{**}P < 0.005$ or $^{***}P < 0.0005$, $n = 6$). (d) and (e) Release profiles of TNFα (d) and MIP-2 (e) after 24 h exposure of J774 macrophages to various concentrations (2, 5, 10, 15, 25, 50 and 100 µgml^{-1}) of pristine (red), partially sulphidated (blue) and completely sulphidated (orange) Ag NPs. This suggests that fully sulphidated nanoparticles inhibited corona formation, thus protected macrophages from nanoparticle toxicity. (Adapted from Miclauş, et al. [154]).

nano-colloidal surface interact strongly with molecules containing monothiol or disulfide groups, partially due to the existence of several possible oxidation states of gold when it is bound to ligands (oxidation states from -I to +V are known). Interestingly, bulk gold is chemically inert and poorly reach to the thiol groups [156]. Gold or silver nanoparticles in biological samples rapidly interact with the thiol-containing proteins, fat or other chemicals, forming a soft corona that, in time, transform into hard corona [157]. Earlier studies have shown that sulphidation decreases toxicity of silver nanoparticles [158-164]. Corona formation onto the silver nanoparticle surface (Figure 22) protects against inflammation (interleukin-1beta, interleukin-6, interleukin-18, tumor necrosis factor alpha (TNFα), and macrophage inflammatory protein 2, Granulocyte-macrophage colony-stimulating factor) [154] (Figure 22).

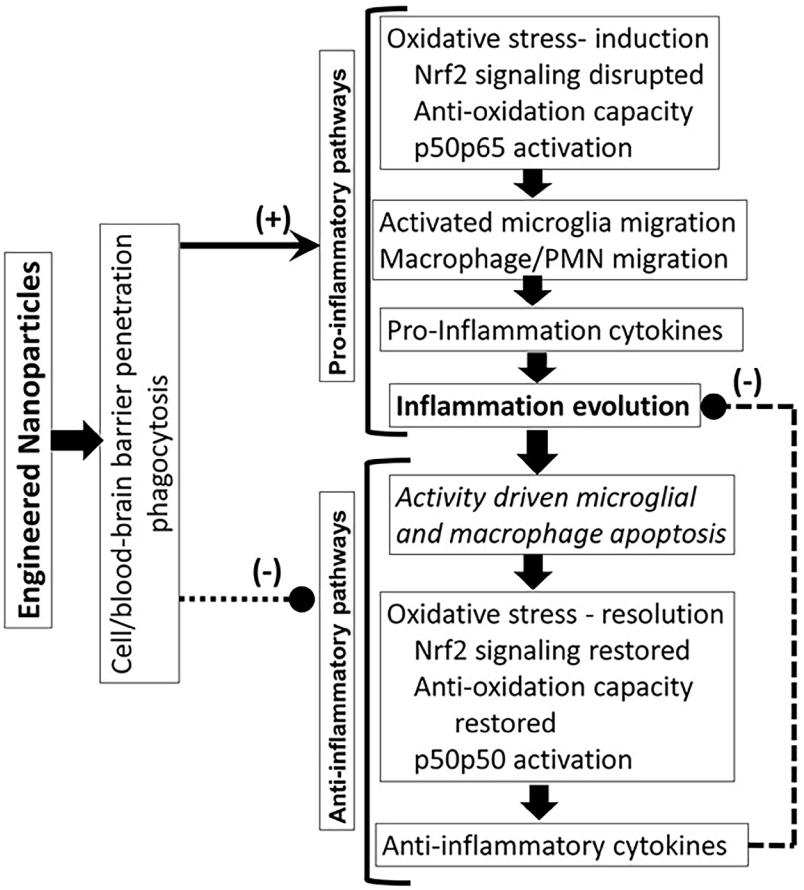

Figure 23: The flow diagram showing mechanisms of action of nanoparticle toxicity.

Mechanisms of nanoparticle toxicity

Humans and animals get exposed to toxins via dermal exposure, ingestion and/or inhalation. Toxin concentrations in the systemic blood depend upon (i) The route of exposure and transfer of the ingested toxin through the membrane barriers, (ii) Metabolism and excretion and (iii) Nonspecific distribution of toxins into different tissues. A very small fraction of the toxin may reach the target site. The toxin-target interaction initiates a series of mechanisms (Figure 23), resulting in an increase in oxidative stress, activation of pro-inflammatory pathways and inhibition of anti-inflammatory pathways, resulting in inflammation dysregulation and cytotoxicity such as necrosis [165-167] DNA damage [168-170] and membrane toxicity [171] (Figure 23).

Conclusions

Nanoparticles, because of their outstanding characteristics and properties, have potential for development of novel nanoparticle-based devices for individualized treatment of alcoholism. Nanoparticles exhibit (i) High surface area to volume ratio, (ii) Surface atoms influencing the particles properties and (iii) Size- and shape-dependent physicochemical properties, quantum confinement (semiconductors), surface Plasmon resonance (some metals) and super-paramagnetism (magnetic particles) [172,173]. Therefore, surface area and/or diameter may influence a nanoparticle's beneficial effects and toxicity [174,175]. Because of the NPs' unique surface and physicochemical properties, they may have therapeutic potential against alcoholism. Unfortunately, the very physicochemical properties that confer the NPs their therapeutic potency also increase their toxicity and adverse effects. Therefore, the therapeutic index of a NP preparation depends on its therapeutic potency/toxicity ratio.

References

1. Cami J, Farre M (2003) Drug addiction. N Engl J Med 349: 975-986.
2. Weiss F, Porrino LJ (2002) Behavioral neurobiology of alcohol addiction: recent advances and challenges. J Neurosci 22: 3332-3337.
3. Sullivan EV, Harris RA, Pfefferbaum A (2010) Alcohol's Effects on Brain and Behavior. Alc Res 33: 127-143.
4. Koob GF, Le Moal M (2006) Neurobiology of Addiction. Elsevier, London.
5. Koob GF (2008) A role for brain stress systems in addiction. Neuron 59: 11-34.

6. Squeglia LM, Jacobus J, Tapert SF (2014) The effect of alcohol use on human adolescent brain structures and systems. Handb Clin Neurol 125: 501-510.

7. Myrick H, Anton RF, Li X, et al. (2004) Differential brain activity in alcoholics and social drinkers to alcohol cues: relationship to craving. Neuropsychopharmacology 29: 393-402.

8. George MS, Anton RF, Bloomer C, et al. (2001) Activation of prefrontal cortex and anterior thalamus in alcoholic subjects on exposure to alcohol-specific cues. Arch Gen Psych 58: 345-352.

9. Di Chiara G (1997) Alcohol and dopamine. Alco Health Res World 21: 108.

10. Blitzer RD, Gil O, Landau EM (1990) Long-term potentiation in rat hippocampus is inhibited by low concentrations of ethanol. Br Res 537: 203-208.

11. Gulya K, Grant KA, Valverius P, et al. (1991) Brain regional specificity and time-course of changes in the NMDA receptor-ionophore complex during ethanol withdrawal. Br Res 547: 129-134.

12. Koob GF (2004) A role for GABA mechanisms in the motivational effects of alcohol. Biochem Pharmacol 68: 1515-1525.

13. Siggins GR, Roberto M, Nie Z (2005) The tipsy terminal: presynaptic effects of ethanol. Pharm Ther 107: 80-98.

14. Woodward JJ (2000) Ethanol and NMDA receptor signaling. Crit Rev Neurobiol 14: 69-89.

15. Grant KA (1995) The role of 5-HT3 receptors in drug dependence. Drug Alc Dependence 38: 155-171.

16. Weinshenker D, Rust NC, Miller NS, et al. (2000) Ethanol-associated behaviors of mice lacking norepinephrine. J Neurosci 20: 3157-3164.

17. Thiele TE, Marsh DJ, Ste Marie L, et al. (1998) Ethanol consumption and resistance are inversely related to neuropeptide Y levels. Nature 396: 366-369.

18. Edwards S, Guerrero M, Ghoneim OM, et al. (2012) Evidence that vasopressin V1b receptors mediate the transition to excessive drinking in ethanol-dependent rats. Addict Biol 17: 76-85.

19. Nam HW, Bruner RC, Choi DS (2013) Adenosine signaling in striatal circuits and alcohol use disorders. Mol Cells 36: 195-202.

20. Berke JD, Hyman SE (2000) Addiction, dopamine, and the molecular mechanisms of memory. Neuron 25: 515-532.

21. Koob GF (2013) Addiction is a Reward Deficit and Stress Surfeit Disorder. Front Psychiatry 4: 72.

22. Gonzales RA, Job MO, Doyon WM (2004) The role of mesolimbic dopamine in the development and maintenance of ethanol reinforcement. Pharmacol Ther 103: 121-146.

23. Starkman BG, Sakharkar AJ, Pandey SC (2012) Epigenetics-beyond the genome in alcoholism. Alcohol Res 34: 293-305.

24. Mann K, Hermann D (2010) Individualized treatment in alcohol-dependent patients. Eur Arch Psychiatry Clin Neurosci 260: 116-120.

25. Kranzler HR, Armeli S, Tennen H, et al. (2011) Double-blind, randomized trial of sertraline for alcohol dependence: moderation by age of onset [corrected] and 5-hydroxytryptamine transporter-linked promoter region genotype. J Clin Psychopharmacol 31: 22-30.

26. Project Match Research Group (1997) Matching alcoholism treatments to client heterogeneity: project MATCH post-treatment drinking outcomes. J Stud Alcohol 58: 7-29.

27. Ashley EA, Butte AJ, Wheeler MT, et al. (2010) Clinical assessment incorporating a personal genome. Lancet 375: 1525-1535.

28. Kim TK, Eberwine JH (2010) Mammalian cell transfection: the present and the future. Anal Bioanal Chem 397: 3173-3178.

29. Singh AK (2015) Engineered Nanoparticles, Structure, Properties and Mechanisms of Toxicity. Elsevier Publication.

30. Gupta A, Main BJ, Taylor BL, et al. (2014) In vitro evaluation of three-dimensional single-walled carbon nanotube composites for bone tissue engineering. J Biomed Mater Res A 102: 4118-4126.

31. Maiti K, Mukherjee K, Gantait A, et al. (2007) Curcumin-phospholipid complex: Preparation, therapeutic evaluation and pharmacokinetic study in rats. International Journal of Pharmaceutics 330: 155-163.

32. Anand P, Kunnumakkara AB, Newman RA, et al. (2007) Bioavailability of curcumin: problems and promises. Mol Pharm 4: 807-818.

33. Singh AK (2014) Challenges in the Medicinal Applications of Carbon Nanotubes (CNTs): Toxicity of the Central Nervous System and Safety Issues. J J Nanomed Nanotech 1: 002.

34. Pokropivny VV, Skorokhod VV (2007) Classification of nanostructures by dimensionality and concept of surface forms engineering in nanomaterial science. Materials Science and Engineering: C 27: 990-993.

35. Thess A, Lee R, Nikolaev P, et al. (1996) Crystalline ropes of metallic carbon nanotubes. Science 273: 483-487.

36. Banholzer MJ (2011) Anisotropic nanomaterials: Synthesis, optical and magnetic properties, and applications. ProQuest, UMI Dissertation Publishing.

37. Baughman RH, Zakhidov AA, de Heer WA (2002) Carbon nanotubes--the route toward applications. Science 297: 787-792.

38. Chatterjee J, Haik Y, Che CJ (2003) Size dependent magnetic properties of iron oxide nanoparticles. Journal of Magnetism and Magnetic Materials 257: 113-118.

39. Rahman IA, Vejayakumaran P, Sipaut CS, et al. (2003) Size-dependent physicochemical and optical properties of silica nanoparticles. Materials Chemistry and Physics 114: 328-332.

40. Biener J, Wittstock A, Baumann TF, et al. (2009) Surface chemistry in nanoscale materials. Materials 2: 2404-2428.

41. Jia M, Lai Y, Tian Z, et al. (2009) Calculation of the surface free energy of fcc copper nanoparticles. Modelling and Simulation in Materials Science and Engineering 17.

42. Nanda KK, Maisels A, Kruis FE, et al. (2003) Higher Surface Energy of Free Nanoparticles. Phys Rev Lett 91: 106102.

43. Bohr N (1923) Structure of Atoms. Nature 112: 29-42.

44. Kramers H, Helge HA (1923) The atomic and Bohr theory of its structure: An elementary presentation. Gyldendal, London.

45. Housecroft C, Sharpe AG (2012) Inorganic chemistry. (4th edn), Pearson.

46. Griffith JS, Orgel LE (1957) Ligand-field theory. Quarterly Reviews, Chemical Society 11: 381-393.

47. Freund HJ (2002) Clusters and islands on oxides: from catalysis via electronics and magnetism to optics. Surface Science 500: 271-299.

48. Scockley W (1950) Electrons and holes in semiconductors. Van Nostrand, Princeton, New Jersy.

49. de Broglie L (1929) The wave nature of the electron. The Nobel Foundation.

50. Davison C, Germer T (1927) The scattering of electrons by a single crystal of nickel. Nature 119: 558-560.

51. Tauc J (1968) Optical properties and electronic structure of amorphous Ge and Si. Materials Research Bulletin 3: 37-46.

52. Agostiano A, Catalano M, Curr ML, et al. (2000) Synthesis and structural characterisation of CdS nanoparticles prepared ina four-components "water-in-oil" microemulsion. Micron 31: 253-258.

53. Akbari B, Tavandashti MP, Zandrahimi M (2011) Particle size characterization of nanoparticles-a practical approach. Iranian Journal of Materials Science & Engineering 8: 48-56.

54. Mohanraj V, Chen Y (2006) Nanoparticles-a review. Tropical Journal of Pharmaceutical Research 5: 561-573.

55. Qi WH, Wang MP (2004) Size and shape dependent melting temperature of metallic nanoparticles. Materials Chemistry and Physics 88: 280-284.

56. Schmid G (2004) Nanoparticles: From Theory to Application, Weinheim, Wiley-VCH.

57. Sun W, Pelletier JC (2007) Efficient conversion of primary and secondary alcohols to primary amines. Tetrahedron Letters 48: 7745-7746.

58. Mu Q, Jiang G, Chen L, et al. (2014) Chemical basis of interactions between engineered nanoparticles and biological systems. Chem Rev 114: 7740-7781.

59. Kralchevsky PA, Nagayama K (2000) Capillary interactions between particles bound to interfaces, liquid films and biomembranes. Adv Colloid Interface Sci 85: 145-192.

60. Nel AE, Mädler L, Velegol D, et al. (2009) Understanding biophysicochemical interactions at the nano-bio interface. Nat mater 8: 543-557.

61. Kukowska-Latallo JF, Bielinska AU, Johnson J, et al. (1996) Efficient transfer of genetic material into mammalian cells using Starburst polyamidoaminedendrimers. Proc Natl Acad Sci USA 93: 4897-4902.

62. Frechet JM (1994) Functional polymers and dendrimers: reactivity, molecular architecture, and interfacial energy. Science 263: 1710-1715.

63. Mourey TH, Turner SR, Rubenstein M, et al. (1992) Unique behaviour of dendritic macromolecules: Intrinsic viscosity of polyether dendrimers. Macromolecules 25: 2401-2406.

64. Klajnert B, Bryszewska M (2001) Dendrimers: properties and applications. Acta Biochimia Polinica 48: 199-208.

65. Lu Y, Shi T, An L, et al. (2010) A simple model for the anomalous intrinsic viscosity of dendrimers. Soft Matter 6: 2619-2622.

66. Koenig S, Müller L, Smith DK (2001) Dendriticbiomimicry: microenvironmental hydrogen-bonding effects on tryptophan fluorescence. Chemistry A European Journal 7: 979-986.

67. Esfand R, Tomalia DA (2001) Poly (amidoamine) (PAMAM) dendrimers: from biomimicry to drug delivery and biomedical applications. Drug Discov Today 6: 427-436.

68. Noriega-Luna B, Godínez LA, Rodríguez FJ, et al. (2014) Applications of Dendrimers in Drug Delivery Agents, Diagnosis, Therapy, and Detection. Journal of Nanomaterials 2014: 507273.

69. Yue Y, Eun JS, Lee MK, et al. (2012) Synthesis and characterization of G5 PAMAM dendrimer containing daunorubicin for targeting cancer cells. Arch Pharm Res 35: 343-349.

70. Fant K, Esbjörner EK, Lincoln P, et al. (2008) DNA condensation by PAMAM dendrimers: self-assembly characteristics and effect on transcription. Biochemistry 47: 1732-1740.

71. Dootz R, Toma AC, Pfohl T (2011) PAMAM6 dendrimers and DNA: pH deACpendent "beads-on-a-string" behavior revealed by small angle X-ray scattering. Soft Matter 7: 8343-8351.

72. Maiti PK, Cagın T, Lin ST, et al. (2005) Effect of Solvent and pH on the Structure of PAMAM Dendrimers. Macromolecules 38: 979-991.

73. Liu Y, Bryantsev VS, Diallo MS, et al. (2009) PAMAM Dendrimers Undergo pH Responsive Conformational Changes without Swelling. J Am Chem Soc 131: 2798-2799.

74. Muller T, Yablon DG, Karchner R, et al. (2002) AFM Studies of High-Generation PAMAM Dendrimers at the Liquid/Solid Interface. Langmuir 18: 7452-7455.

75. Nanjwade BK, Bechra HM, Derkar GK, et al. (2009) Emerging polymers for drug-delivery systems. Eur J Pharm Sci 38: 185-196.

76. Wang DJ, Imae T (2004) Fluorescence emission from Dendrimer& its pH dependence. J Am Chem Soc 126: 13204-13205.

77. Ottaviani MF, Sacchi B, Turro NJ, et al. (1999) An EPR study of the interactions between starburst dendrimers and polynucleotides. Macromolecules 32: 2275-2282.

78. Ajayan PM (1999) Nanotubes from carbon. Chem Rev 99: 1787-1800.

79. Dresselhaus MS, Dresselhaus G, Eklund PC (1996) Science of Fullerenes and Carbon Nanotubes. J Am Chem Soc 118: 8987.

80. Dresselhaus MS, Dresselhaus G, Avouris P (2001) Carbon nanotubes: Synthesis, Structure, Properties and Applications. Springer Berlin Heidelberg 80.

81. Moniruzzaman M, Winey KI (2006) Polymer nanocomposites containing carbon nanotubes. Macromolecules 39: 5194-5205.

82. Saito R, Dresselhaus G, Dresselhaus MS (1998) Physical properties of carbon nanotubes. Imperial College Press, London, UK.

83. Saito R, Dresselhaus G, Dresselhaus MS (2000) Trigonal warping effect of carbon nanotubes. Physical Review B 61: 2981-2990.

84. Tian F, Cui D, Schwarz H, et al. (2006) Cytotoxicity of single-wall carbon nanotubes on human fibroblasts. Toxicol In Vitro 20: 1202-1212.

85. Issa B, Obaidat IM, Albiss BA (1999) Magnetic nanoparticles. J Magnetism Magnetic Materials 200: 359-372.

86. Issa B, Obaidat IM, Albiss BA (2013) Magnetic Nanoparticles: Surface Effects and Properties Related to Biomedicine Applications. Int J Mol Sci 14: 21266-21305.

87. Kodama RH (1999) Magnetic nanoparticles. Journal of Magnetism and Magnetic Materials 200: 359-372.

88. Bagwe RP, Yang C, Hilliard LR, et al. (2004) Optimization of dye-doped silica nanoparticles prepared using a reverse microemulsion method. Langmuir 20: 8336-8342.

89. Bhatt N, Huang PJ, Dave N, et al. (2011) Dissociation and Degradation of Thiol-Modified DNA on Gold Nanoparticles in Aqueous and Organic Solvents. Langmuir 27: 6132-6137.

90. Chompoosor A, Han G, Rotello VM (2008) Charge Dependence of Ligand Release and Monolayer Stability of Gold Nanoparticles by Biogenic Thiols. Bioconjug Chem 19: 1342-1345.

91. Herdt AR, Kim BS, Taton TA (2007) Encapsulated magnetic nanoparticles as supports for proteins and recyclable biocatalysts. Bioconjug Chem 18: 183-189.

92. Hong R, Han G, Fernández JM, et al. (2006) Glutathione-Mediated Delivery and Release Using Monolayer Protected Nanoparticle Carriers. J Am Chem Soc 128: 1078-1079.

93. Kassam A, Bremner G, Clark B, et al. (2006) Place Exchange Reactions of Alkyl Thiols on Gold Nanoparticles. J Am Chem Soc 128: 3476-3477.

94. Klajn R, Bishop KJM, Fialkowski M, et al. (2007) Plastic and Moldable Metals by Self-Assembly of Sticky Nanoparticle Aggregates. Science 316: 261-264.

95. Mai J, Waisman DM, Sloane BF (2000) Cell surface complex of cathepsin B/annexin II tetramer in malignant progression. Biochim Biophys Acta 1477: 215-230.

96. Guarise C, Pasquato L, Scrimin P (2005) Reversible aggregation/deaggregation of gold nanoparticles induced by a cleavable dithiol linker. Langmuir 21: 5537-5541.

97. Santi DV, Schneider EL, Reid R, et al. (2012) Predictable and tunable half-life extension of therapeutic agents by controlled chemical release from macromolecular conjugates. Proc Natl Acad Sci USA 109: 6211-6216.

98. Calderon M, Graeser R, Kratz F, et al. (2009) Development of enzymatically cleavable prodrugs derived from dendritic polyglycerol. Bioorg Med Chem Lett 19: 3725-3728.

99. Klajn R, Browne KP, Soh S, et al. (2010) Nanoparticles That "Remember" Temperature. Small 6: 1385-1387.

100. Elbaz J, Cecconello A, Fan Z, et al. (2013) Powering the programmed nanostructure and function of gold nanoparticles with catenated DNA machines. Nat Commun 4: 2000.

101. Hua M, Jiang Y, Wu B, et al. (2013) Fabrication of a new hydrous Zr(IV) oxide-based nanocomposite for enhanced Pb(II) and Cd(II) removal from waters. ACS Appl Mater Interfaces 5: 12135-12142.

102. Sannohe Y, Sugiyama H (2010) Overview of Formation of G-Quadruplex Structures. Current Protocols in Nucleic Acid Chemistry, John Wiley & Sons, Inc.

103. Sannohe Y, Sugiyam H (2012) Single strand DNA catenane synthesis using the formation of G-quadruplex structure. Bioorg Med Chem 20: 2030-2034.

104. Saji VS, Choe HC, Yeung KWK (2010) Nanotechnology in Biomedical Applications: a review. Int J Nano and Biomaterials 3: 119-139.

105. Moghimi SM (2006) Recent developments in polymeric nanoparticle engineering and their applications in experimental and clinical oncology. Anticancer Agents Med Chem 6: 553-561.

106. Zolata H, Afarideh H, Davani FA (2016) Triple Therapy of HER2+ Cancer Using Radiolabeled Multifunctional Iron Oxide Nanoparticles and Alternating Magnetic Field. Cancer Biother Radiopharm 31: 324-329.

107. Dhawan U, Wang SM, Chu YH, et al. (2016) Nanochips of Tantalum Oxide Nanodots as artificial-microenvironments for monitoring Ovarian cancer progressiveness. Scientific Reports 6.

108. Gorjikhah F, Davaran S, Salehi RA, et al. (2016) Improving "lab-on-a-chip" techniques using biomedical nanotechnology: a review. Artif Cells Nanomed Biotech 44: 1609-1614.

109. Yu J, Yang Y, Seiffert-Sinha K, et al. (2016) Multi-layer coated nanorobot end-effector for efficient drug delivery. Nanotechnology (IEEE-NANO), 2016 IEEE 16th International Conference on IEEE, 511-514.

110. Zhang XD, Wu D, Shen X, et al. (2011) Size-dependent in vivo toxicity of PEG-coated gold nanoparticles. Int J Nanomedicine 6: 2071-2081.

111. Chinnadayyala SR, Santhosh M, Singh NK, et al. (2015) Alcohol oxidase protein mediated in-situ synthesized and stabilized gold nanoparticles for developing amperometric alcohol biosensor. Biosens Bioelectron 69: 155-161.

112. Gómez-Anquela C, García-Mendiola T, Abad JM, et al. (2015) Scaffold electrodes based on thioctic acid-capped gold nanoparticles coordinated Alcohol Dehydrogenase and Azure A films for high performance biosensor. Bioelectrochemistry 106: 335-342.

113. Luo P, Xie G, Liu Y, et al. (2008) Electrochemical detection of blood alcohol concentration using a disposable biosensor based on screen-printed electrode modified with Nafion and gold nanoparticles. Clin Chem Lab Med 46: 1641-1647.

114. Averbakh AZ, Pekel ND, Seredenko VI, et al. (1995) Flavin-dependent alcohol oxidase from the yeast Pichiapinus. Spatial localization of the coenzyme FAD in the protein structure: hot-tritium bombardment and ESR experiments. Biochem J 310: 601-604.

115. Barry RE, McGivan JD (1985) Acetaldehyde alone may initiate hepatocellular damage in acute alcoholic liver disease. Gut 26: 1065-1069.

116. Vyas TK, Tiwari SB, Amiji MM (2006) Formulation and physiological factors influencing CNS delivery upon intranasal administration. Crit Rev Ther Drug Carrier Syst 23: 319-347.

117. Emerich DF, Thanos CG (2006) The pinpoint promise of nanoparticle-based drug delivery and molecular diagnosis. Biomol Eng 23: 171-184.

118. Yin W, Akala EO Taylor RE (2002) Design of naltrexone-loaded hydrolyzablecrosslinked nanoparticles. Int J Pharm 244: 9-19.

119. Banks SL, Pinninti RR, Gill HS, et al. (2010) Transdermal delivery of naltrexol and skin permeability lifetime after microneedle treatment in hairless guinea pigs. J Pharm Sci 99: 3072-3080.

120. Sharma HS, Ali SF, Dong W, et al. (2007) Drug delivery to the spinal cord tagged with nanowire enhances neuroprotective efficacy and functional recovery following trauma to the rat spinal cord. Ann N Y Acad Sci 1122: 197-218.

121. Green-Sadan T, Kuttner Y, Lublin-Tennenbaum T, et al. (2005) Glial cell line-derived neurotrophic factor-conjugated nanoparticles suppress acquisition of cocaine self-administration in rats. Exp Neurol 194: 97-105.

122. Carnicella S, Amamoto R, Ron D (2009) Excessive alcohol consumption is blocked by glial cell line-derived neurotrophic factor. Alcohol 43: 35-43.

123. Rao P, Yallapu MM, Sari Y, et al. (2015) Designing novel nanoformulations targeting glutamate transporter excitatory amino acid transporter 2: Implications in treating drug addiction. J Pers Nanomed 1: 3-9.

124. Tykhomyrov AA, Nedzvetsky VS, Klochkov VK, et al. (2008) Nanostructures of hydrated C60 fullerene (C60HyFn) protect rat brain against alcohol impact and attenuate behavioral impairments of alcoholized animals. Toxicology 246: 158-165.

125. Andrievsky G, Klochkov V, Derevyanchenko L (2005) Is the C60 fullerene molecule toxic? Fullerenes, Nanotubes, and Carbon Nanostructures 13: 363-376.

126. Sharma V, Park K, Srinivasarao M (2009) Colloidal Dispersion of Gold Nanorods: Historical Background, Optical Properties, Seed-Mediated Synthesis, Shape Separation and Self-Assembly. Materials Science and Engineering: R: Reports 65: 1-38.

127. Merza KS, Al-Attabi HD, Abbas ZM, et al. (2012) Comparative Study on Methods for Preparation of Gold Nanoparticles. Green and Sustainable Chemistry 2: 26-28.

128. Kumar KP, Paul W, Sharma CP (2011) Green synthesis of gold nanoparticles with Zingiberofficinaleextract: Characterization and blood compatibility. Process Biochemistry 46: 2007-2013.

129. Nellore J, Pauline C, Amarnath K, et al. (2012) Antioxidant effect of gold nanoparticles synthesised from curcuma longa restrains 1-methyl-2-phenyl pyridinium ion induced stress in PC12 cells. Journal of Nanoneuroscience 2: 63-74.

130. Kora AJ, Beedu SR, Jayaramn A (2012) Size-controlled green synthesis of silver nanoparticles mediated by gum ghatti (Anogeissuslatifolia) and its biological activity. Org Med Chem Lett 2: 17.

131. Duan H, Wang D, Li Y (2015) Green chemistry for nanoparticle synthesis. Chem Soc Rev 44: 5778-5792.

132. Shah M, Fawcett D, Sharma S, et al. (2015) Green synthesis of metallic nanoparticles via biological entities. Materials 8: 7278-7308.

133. Anjum S, Abbasi BH, Shinwari ZK (2016) Plant-mediated green synthesis of sliver nanoparticles for biomedical applications: Challenges and Opportunities. Pak J Bot 48: 1731-1760.

134. Chung IM, Park I, Seung-Hyun K, et al. (2016) Plant-mediated synthesis of silver nanoparticles: their characteristic properties and therapeutic applications. Nanoscale Res Lett 11: 40.

135. Singh AK, Jiang Y, Gupta S, et al. (2013) Anti-inflammatory potency of nano-formulated puerarin and curcumin in rats subjected to the lipopolysaccharide-induced inflammation. J Med Food 16: 899-911.

136. Mura S, Nicolas J, Couvreur P (2013) Stimuli-responsive nanocarriers for drug delivery. Nature Materials 12: 991-1003.

137. Kaushik A, Jayant RD, Sagar V, et al. (2014) The potential of magneto-electric nanocarriers for drug delivery. Expert Opin Drug Deliv 11: 1635-1646.

138. Argyo C, Weiss V, Bräuchle C, et al. (2013) Multifunctional mesoporous silica nanoparticles as a universal platform for drug delivery. Chemistry of Materials 26: 435-451.

139. Oberdörster G, Oberdörster E, Oberdörster J (2007) Concepts of Nanoparticle Dose Metric and Response Metric. Environ Health Perspect 115: 290.

140. Maynard AD, Kuempel E (2005) Airborne nanostructured particles and occupational health. Journal of Nanoparticle Research 7: 587-614.

141. Duffin R, Tran L, Brown D, et al. (2007) Proinflammogenic effects of low-toxicity and metal nanoparticles in vivo and in vitro: highlighting the role of particle surface area and surface reactivity. Inhal Toxicol 19: 849-856.

142. Castranova V (2011) Overview of current toxicological knowledge of engineered nanoparticles. J Occup Environ Med 53.

143. Oberdörster G, Oberdörster E, Oberdörster J (2005) Nanotoxicology: an emerging discipline evolving from studies of ultrafine particles. Environ Health Perspect 113: 823-839.

144. Teeguarden JG, Hinderliter PM, Orr G, et al. (2007) Particokinetics in vitro: dosimetry considerations for in vitro nanoparticle toxicity assessments. Toxicol Sci 95: 300-312.

145. Jiang J, Oberdörster G, Elder A, et al. (2008) Does nanoparticle activity depend upon size and crystal phase? Nanotoxicology 2: 33-42.

146. Hussain S, Boland S, Baeza-Squiban A, et al. (2009) Oxidative stress and proinflammatory effects of carbon black and titanium dioxide nanoparticles: role of particle surface area and internalized amount. Toxicology 260: 142-149.

147. Hedwig MB, Margriet VDZP, Ilse Gosens, et al. (2014) Physicochemical characteristics of nanomaterials that affect pulmonary inflammation. Particle and Fibre Toxicology 11: 18.

148. Oberdörster G, Sharp Z, Atudorei V, et al. (2004) Translocation of inhaled ultrafine particles to the brain. Inhal Toxicol 16: 437-445.

149. Wittmaack K (2007) In search of the most relevant parameter for quantifying lung inflammatory response to nanoparticle exposure: particle number, surface area, or what? Environ Health Perspect 115: 187-194.

150. Van Ravenzwaay B, Landsiedel R, Fabian E, et al. (2009) Comparing fate and effects of three particles of different surface properties: nano-TiO(2), pigmentaryTiO(2) and quartz. Toxicol Lett 186: 152-159.

151. Schmid O, Stieger T (2016) Surface area is the biologically most effective dose metric for acute nanoparticle toxicity in the lung. Journal of Aerosol Science 99: 133-143.

152. Zanganeh S, Spitler R, Erfanzadeh M, et al. (2016) Protein corona: opportunities and challenges. Int J Biochem Cell Biol 75: 143-147.

153. Tenzer S, Docter D, Kuharev J, et al. (2013) Rapid formation of plasma protein corona critically affects nanoparticle pathophysiology. Nature Nanotechnology 8: 772-781.

154. Miclăuş T, Beer C, Chevallier J, et al. (2016) Dynamic protein coronas revealed as a modulator of silver nanoparticle sulphidation in vitro. Nat Commun 7: 11770.

155. Haruta M (2007) When gold is not noble: catalysis by nanoparticles. Chem Res 3: 75-87.

156. Casals E, Pfaller T, Duschl A, et al. (2010) Time evolution of the nanoparticle protein corona. ACS Nano 4: 3623-3632.

157. Bowles KC, Bianchini A, Brauner CJ, et al. (2002) Evaluation of the effect of reactive sulfide on the acute toxicity of silver (I) to Daphnia magna. Part 1: Description of the chemical system. Environmental Toxicology and Chemistry 21: 1286-1293.

158. Bianchini A, Bowles KC, Brauner CJ, et al. (2002) Evaluation of the effect of reactive sulfide on the acute toxicity of silver (I) to Daphnia magna. part 2: Toxicity results. Environ Toxicol Chem 21: 1294-1300.

159. Choi O, Clevenger TE, Deng B, et al. (2009) Role of sulfide and ligand strength in controlling nanosilver toxicity. Water Res 43: 1879-1886.

160. Levard C, Hotze EM, Colman BP, et al. (2013) Sulfidation of silver nanoparticles: natural antidote to their toxicity. Environ Sci Technol 47: 13440-13448.

161. Lee YK, Choi EJ, Webster TJ, et al. (2015) Effect of the protein corona on nanoparticles for modulating cytotoxicity and immunotoxicity. Int J Nanomedicine 10: 97-113.

162. Cai H, Ma Y, Wu Z, et al. (2016) Protein corona influences liver accumulation and hepatotoxicity of gold nanorods. NanoImpact 3-4: 40-46.

163. Drieben Marc D (2016) Investigation of nanoparticle toxicity: Characterization of protein corona and evaluation of oxidative stress by protein carbonylation. Doctoral dissertation, Freie Universität Berlin.

164. Mazzolini J, Weber RJ, Chen HS, et al. (2016) Protein Corona Modulates Uptake and Toxicity of Nanoceria via Clathrin-Mediated Endocytosis. Biol Bull 231: 40-60.

165. Lopez T, Figueras F, Manjarrez J, et al. (2010) Catalytic nanomedicine: a new field in antitumor treatment using supported platinum nanoparticles. In vitro DNA degradation and in vivo tests with C6 animal model on Wistar rats. Eur J Med Chem 45: 1982-1990.

166. Loh JW, Yeoh G, Saunders M, et al. (2010) Uptake and cytotoxicity of chitosan nanoparticles in human liver cells. Toxicol Appl Pharmacol 249: 148-157.

167. Abdelhalim MA, Jarrar BM (2012) Histological alterations in the liver of rats induced by different gold nanoparticle sizes, doses and exposure duration. J Nanobiotechnology 10: 5.

168. Yang L, Gordon VD, Mishra A, et al. (2007) Synthetic antimicrobial oligomers induce a composition-dependent topological transition in membranes. J Am Chem Soc 129: 12141-12147.

169. Lipovsky A, Tzitrinovich Z, Friedmann H, et al. (2009) EPR Study of Visible Light-Induced ROS Generation by Nanoparticles of ZnO. J Phys Chem C 113: 15997-16001.

170. Shen Q, Nie Z, Guo M, et al. (2009) Simple and rapid colorimetric sensing of enzymatic cleavage and oxidative damage of single-stranded DNA with unmodified gold nanoparticles as indicator. Chem Commun 28: 929-931.

171. Stern PC, Fineberg HV (1996) Understanding risk: informing decisions in a democratic society. Committee on Risk Characterization, Commission on Behavioral and Social Sciences and Education, National Research Council, Washington, DC.

172. Nel A, Xia T, Li N, et al. (2006) Toxic potential of materials at the nanolevel. Science 311: 622-627.

173. Khanna L, Verma NK (2013) Size-dependent magnetic properties of calcium ferrite nanoparticles. Journal of Magnetism and Magnetic Materials 336: 1-7.

174. Ahmadi M, Ghasemi MR, Rafsanjani HH (2011) Study of Different Parameters in TiO2 Nanoparticles Formation. J Mat Sci Eng 5: 87-93.

175. Gliga AR, Skoglund S, Wallinder IO, et al. (2014) Size-dependent cytotoxicity of silver nanoparticles in human lung cells: the role of cellular uptake, agglomeration and Ag release. Part Fibre Toxicol 11: 11.

176. Goldstein AN, Echer CM, Alivisatos AP (1992) Melting in semiconductor nanocrystals. Science 256: 1425-1427.

177. Lu HM, Jiang Q (2004) Size-Dependent Surface Energies of Nanocrystals. J Phys Chem B 108: 5617-5619.

178. Dubiel M, Hofmeister H, Schurig E (1997) Compressive stresses in Ag nanoparticle doped glasses by ion implantation. Physica Status Solidi (b) 203: 5-6.

179. Montano PA, Schulze W, Tesche B, et al. (1984) Extended x-ray-absorption fine-structure study of Ag particles isolated in solid argon. Physical Review B 30: 672-677.

180. Lasagna-Reeves C, Gonzalez-Romero D, Barria MA, et al. (2010) Bioaccumulation and toxicity of gold nanoparticles after repeated administration in mice. Biochem Biophys Res Commun 393: 649-655.

181. Shah NB, Vercellotti GM, White JG, et al. (2012) Blood-nanoparticle interactions and in vivo biodistribution: impact of surface PEG and ligand properties. Mol Pharm 9: 2146-2155.

182. Morones JR, Elechiguerra JL, Camacho A, et al. (2005) The bactericidal effect of silver nanoparticles. Nanotechnology 16: 2346-2353.

183. Kim S, Choi JE, Choi J, et al. (2009) Oxidative stress-dependent toxicity of silver nanoparticles in human hepatoma cells. Toxicol In Vitro 23: 1076-1084.

184. Asharani PV, Wu YL, Gong ZY, et al. (2008) Toxicity of silver nanoparticles in zebrafish models. Nanotechnology 19: 255102.

185. García-Barrasa J, López-de-Luzuriaga JM, Monge M (2011) Silver nanoparticles: synthesis through chemical methods in solution and biomedical applications. Central Eur J Chem 9: 7-19.

186. Wang BX, Zhao Y, Zhao XP (2007) The wettability, size effect and electrorheological activity of modified titanium oxide nanoparticles. Colloids and Surfaces A-Physicochemical and Engineering Aspects 295: 27-33.

187. Omura Y, Lu D, Jones MK, et al. (2015) Early Detection of Autism (ASD) by a Non-invasive Quick Measurement of Markedly Reduced Acetylcholine & DHEA and Increased β-Amyloid (1-42), Asbestos (Chrysotile), Titanium Dioxide, Al, Hg & often Coexisting Virus Infections (CMV, HPV 16 and 18), Bacterial Infections etc. in the Brain and Corresponding Safe Individualized Effective Treatment. Acupunct Electrother Res 40: 157-187.

188. Wu WH, Sun X, Yu YP, et al. (2008) TiO2 nanoparticles promote beta-amyloid fibrillation in vitro. Biochem Biophys Res Commun 373: 315-318.

189. Keenan CR, Goth-Goldstein R, Lucas D, et al. (2009) Oxidative stress induced by zero-valent iron nanoparticles and Fe(II) in human bronchial epithelial cells. Environ Sci Technol 43: 4555-4560.

190. Gao B, Sinha S, Fleming L, et al. (2001) Alloy formation in nanostructured silicon. Advanced Materials 13: 816-819.

191. Singh N, Jenkins GJ, Asadi R, et al. (2010) Potential toxicity of superparamagnetic iron oxide nanoparticles (SPION). Nano Rev 1.

192. Donaldson K, Aitken R, Tran L, et al. (2006) Carbon nanotubes: a review of their properties in relation to pulmonary toxicology and workplace safety. Toxicol Sci 92: 5-22.

193. Lam CW, James JT, McCluskey R, et al. (2006) A review of carbon nanotube toxicity and assessment of potential occupational and environmental health risks. Crit Rev Toxicol 36: 189-217.

194. Firme CP, Bandaru PR (2010) Toxicity issues in the application of carbon nanotubes to biological systems. Nanomedicine 6: 245-256.

195. Partha R, Conyers JL (2009) Biomedical applications of functionalized fullerene-based nanomaterials. Int J Nanomedicine 4: 261-275.

196. Kolosnjaj J, Szwarc H, Moussa F (2007) Toxicity studies of fullerenes and derivatives. Adv Exp Med Biol 620: 168-180.

197. Elsabahy M, Wooley KL (2013) Cytokines as biomarkers of nanoparticle immunotoxicity. Chem Soc Rev 42: 5552-5576.

198. Kumari A, Yadav SK, Yadav SC (2010) Biodegradable polymeric nanoparticles based drug delivery systems. Colloids and Surfaces B: Biointerfaces 75: 1-18.

199. Fischer M, Vogtle F (1999) Dendrimers: from design to application-a progress report. Angewandte Chemie International Edition 38: 884-905.

200. Menjoge AR, Kannan RM, Tomalia DA (2010) Dendrimer-based drug and imaging conjugates: design considerations for nanomedical applications. Drug Discov Today 15: 171-185.

201. Dobrovolskaia MA, Patri AK, Simak J, et al. (2011) Nanoparticle size and surface charge determine effects of PAMAM dendrimers on human platelets in vitro. Mol Pharm 9: 382-393.

202. Máté Z, Horváth E, Kozma G, et al. (2016) Size-Dependent Toxicity Differences of Intratracheally Instilled Manganese Oxide Nanoparticles: Conclusions of a Subacute Animal Experiment. Biol Trace Elem Res 171: 156-166.

203. Vanderschuren LJ, Everitt BJ (2005) Behavioral and neural mechanisms of compulsive drug seeking. Eur J Pharmacol 526: 77-88.

204. Brust M, Kiely CJ (2002) Some recent advances in nanostructure preparation from gold and silver particles: a short topical review. Colloids and Surfaces A: Physicochemical and Engineering Aspects 202: 175-186.

205. http://www.organic-chemistry.org/namedreactions/

206. Roberts MJ, Kozlowski A (2002) Hydroxyapatite-targeting poly (ethylene glycol) and related polymers. Shearwater Corporation, U.S. Patent.

207. Love LJ, Jansen JF, McKnight TE, et al. (2005) Ferrofluid field induced flow for microfluidic applications. IEEE/ASME Transactions on Mechatronics 10: 68-76.

208. Aryal S, Grailer JJ, Pilla S, et al. (2009) Doxorubicin conjugated gold nanoparticles as water-soluble and pH-responsive anticancer drug nanocarriers. J Mater Chem 19: 7879-7884.

209. Liu Y, Du J, Yan M, et al. (2013) Biomimetic enzyme nanocomplexes and their use as antidotes and preventive measures for alcohol intoxication. Nature Nanotechnology 8: 187-192.

210. Singh A (2017) Critical Review of Alcohol, Alcoholism and the Withdrawal Symptoms II. Sci J Addiction and Rehab In Press.

211. Benlhabib E, Baker JI, Keyler DE, et al. (2004) Effects of purified puerarin on voluntary alcohol intake and alcohol withdrawal symptoms in P rats receiving free access to water and alcohol. J Med Food 7: 180-186.

212. Benlhabib E, Baker JI, Keyler DE, et al. (2004) Kudzu root extract suppresses voluntary alcohol intake and alcohol withdrawal symptoms in P rats receiving free access to water and alcohol. J Med Food 7: 168-179.

213. Nair M, Guduru R, Liang P, et al. (2013) Externally controlled on-demand release of anti-HIV drug using magneto-electric nanoparticles as carriers. Nature Communications 4.

214. Sagar V, Pilakka-Kanthikeel S, Pottathil R, et al. (2014) Towards nanomedicines for neuroAIDS. Rev Med Virol 24: 103-124.

215. Oberdörster G, Ferin J, Lehnert BE (1994) Correlation between particle size, in vivo particle persistence, and lung injury. Environ Health Perspect 102: 173-179.